

## CHAPTER IV

### RESULTS AND DISCUSSION

#### 4.1 Determination of coated column performance

The qualities of the columns prepared in this study were evaluated by means of Grob test [41-42]. Test chromatograms obtained from OV-1701, BSiMe, and BSiAc columns are depicted in figures 4.1-4.3 respectively. The test mixtures are composed of decane (**C**<sub>10</sub>), undecane (**C**<sub>11</sub>), nonanal (**al**), 1-octanol (**ol**), 2,3-butanediol (**D**), 2,6-dimethylaniline (**A**), 2,6-dimethylphenol (**P**), 2-ethylhexanoic acid (**S**), dicyclohexylamine (**am**), and methyl esters of fatty acids C<sub>10</sub> – C<sub>12</sub> (**E**<sub>10</sub> – **E**<sub>12</sub>). These substances provide the following information on column characteristics: separation efficiency measured from the average TZ value of ester peaks (**E**<sub>10</sub> – **E**<sub>12</sub>), inertness observed from the adsorption of alcohols (**ol** and **D**) and aldehyde (**al**), together with acidity and basicity evaluated from the adsorption of acids and bases (**A**, **P**, **S**, and **am**).

According to figure 4.1, OV-1701 column has fairly high separation efficiency (an average TZ value of 42.73). Moreover, this column is suitable for the quantitative analyses of monoalcohols because of no adsorption of **ol**. However, **D** and **al** are slightly adsorbed, indicating that the separations of alcohols other than monoalcohols and of aldehydes may not be appropriate. Considering **P** and **A** peaks, they are rather equivalent which indicates the neutrality of the column. Nevertheless, OV-1701 column is very active to strong acid (**S**) and strong base (**am**); therefore, underivatized carboxylic acids and amines cannot be analyzed on this phase.

As shown in figure 4.2, the efficiency of BSiMe column is rather high (an average TZ value of 43.66). No adsorption of **ol** is observed; however, **D** and **al** are moderately adsorbed. Thus, this column is inert to monoalcohols but active to alcohols with more than one hydroxyl group and aldehydes. Moreover, adsorption of weak acid (**P**) and weak base (**A**) is very low (nearly 100% eluted), and both of them are virtually equivalent. This means that the column is neutral. Nonetheless, the peaks of **S** and **am** are extremely low; consequently, BSiMe column is unsuitable for the

separation of underivatized carboxylic acids and amines. Interestingly, **D** and **S**, which are chiral compounds, showed the indication of separation of enantiomers.

For BSiAc column (figure 4.3), the separation efficiency is still high (an average TZ value of 40.59). Despite neutrality, this column is severely active to alcohols (**ol**, **D**) as well as strong acid (**S**) and base (**am**), all peaks of which are absent or poorly eluted. In turn, BSiAc column is extremely not suitable for the separation of alcohols, carboxylic acids and amines. Nevertheless, it can be used for the analysis of esters, the compounds of interest in this study. In addition, it may offer different selectivity from BSiMe column, as seen from the difference in elution order of **ol**, **al**, **A**, and **P** peaks.

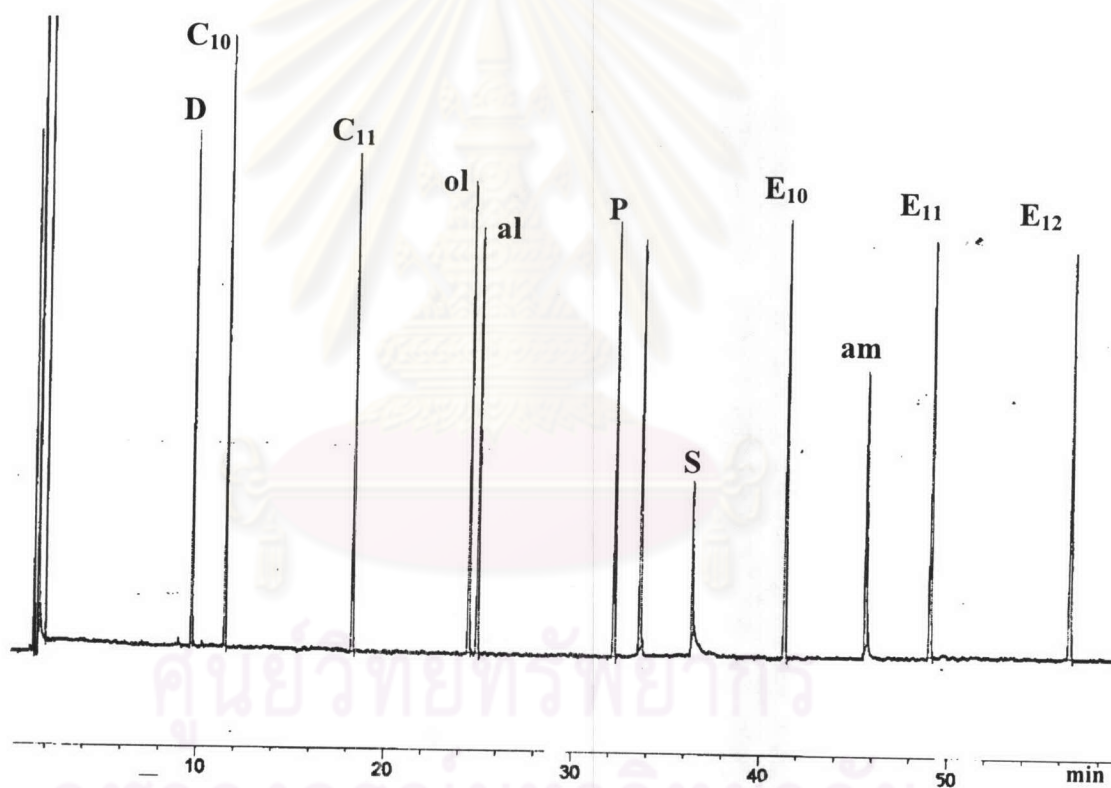


Figure 4.1 Chromatogram of Grob test on OV-1701 column (32.38 m  $\times$  0.25 mm i.d.  $\times$  0.25  $\mu$ m film thickness); temperature program: 40  $^{\circ}$ C to 160  $^{\circ}$ C at 1.54  $^{\circ}$ C/min

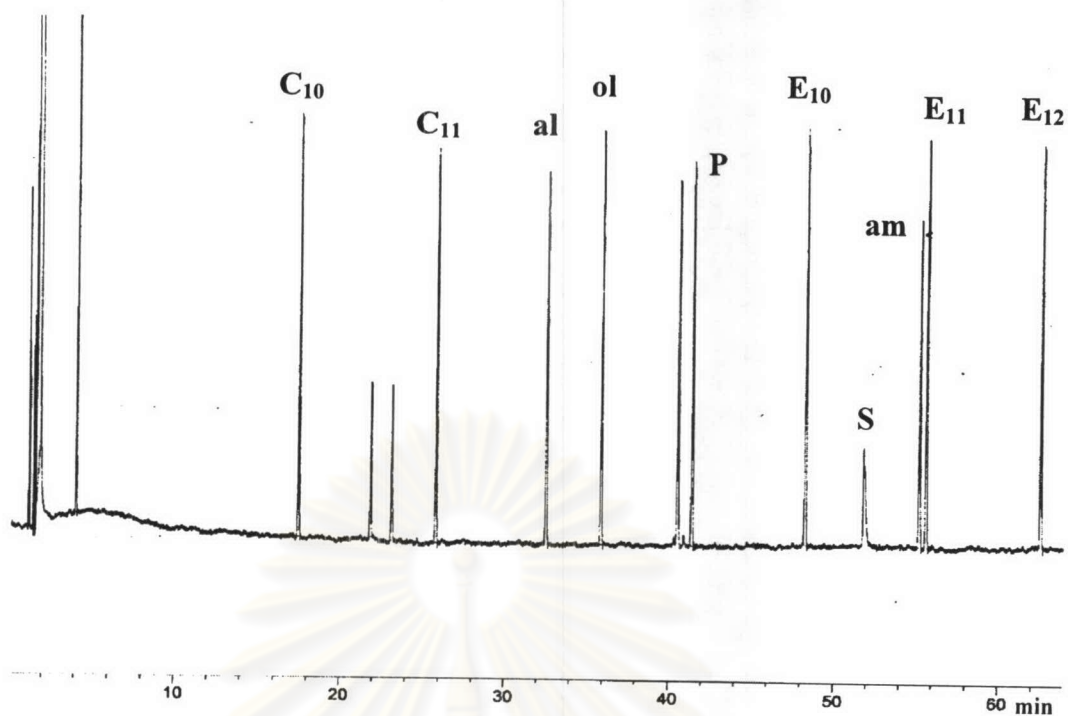


Figure 4.2 Chromatogram of Grob test on BSiMe column (31.8 m × 0.25 mm i.d. × 0.25 μm film thickness); temperature program: 40 °C to 160 °C at 1.57 °C/min

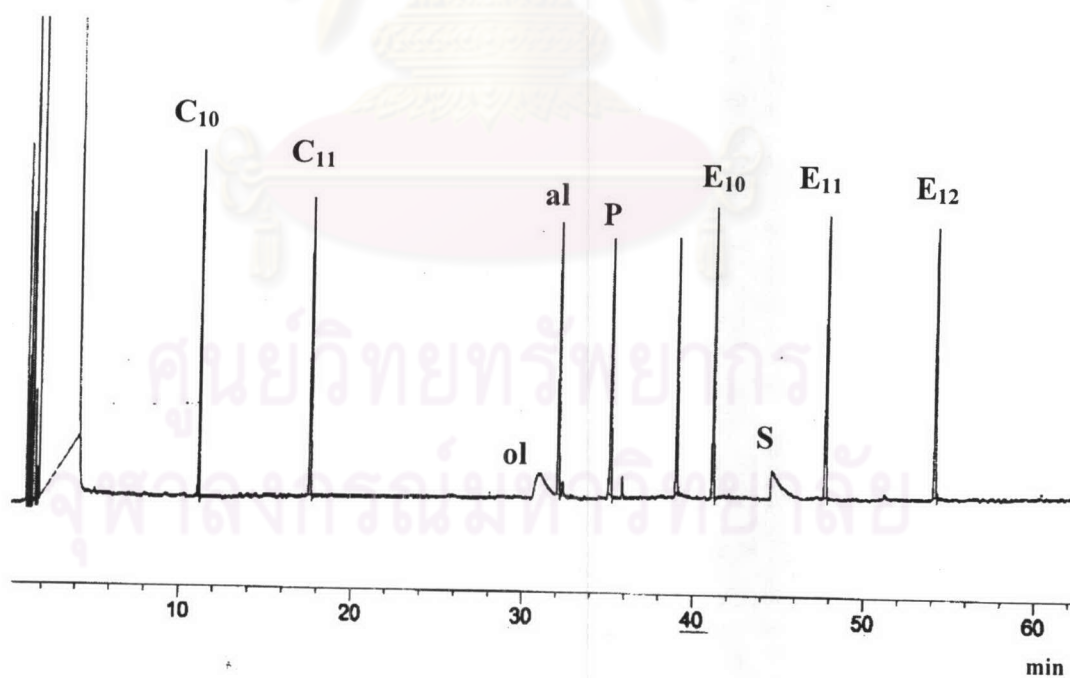


Figure 4.3 Chromatogram of Grob test on BSiAc column (30.24 m × 0.25 mm i.d. × 0.25 μm film thickness); temperature program: 40 °C to 160 °C at 1.65 °C/min



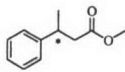
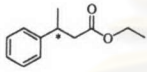
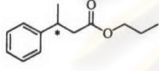
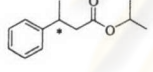
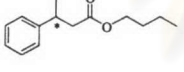
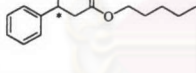
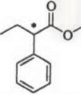
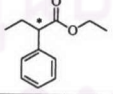
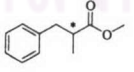
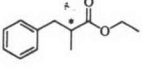
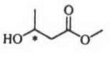
## 4.2 Gas chromatographic separation results

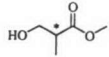
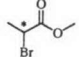
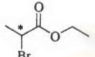
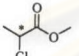
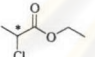
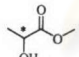
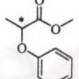
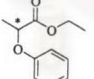
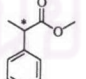
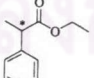
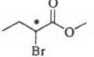
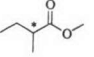
The separation results of all esters with different substitution patterns are presented in table 4.1, in which the retention and separation factors for each chiral ester on three columns (OV-1701, BSiMe, and BSiAc columns) are compared at the same temperature. On account of peak tailing effect, the chromatographic results of **M15-Me**, **M16-Me**, **M7-Me**, and **M7-Et** on BSiAc column were not obtainable. All esters showed higher retention ( $k'$ ) on the two chiral columns than on the nonchiral OV-1701 column. Moreover, all esters could be separated into their enantiomers over a part of temperature range examined and on at least one chiral column used. Evidently, analyte structure plays a key role in enantioseparation: esters with different substitution patterns, e.g. alkyl chain length, position of substituent, and type of substituent, exhibit clear differences in retention and enantioselectivity. For most esters, retention factors substantially increased with lengthening ester chain while separation factors slightly decreased. However, there are some exceptions for a few groups of esters, e.g. separation factors of **M7-R** and **M20-R** on BSiMe phase increased with increasing ester chain length while those of **M6-R** did not change much.

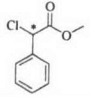
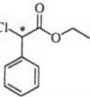
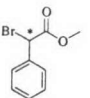
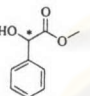
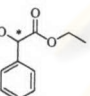
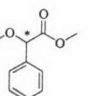
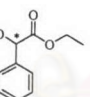
ศูนย์วิจัยทรัพยากร  
จุฬาลงกรณ์มหาวิทยาลัย



Table 4.1 Retention factors ( $k'$ ) and separation factors ( $\alpha$ ) of chiral esters with different substitution patterns on three different stationary phases

| compound       | structure   | temp.(°C) | OV-1701 | BSiMe  |          | BSiAc  |          |
|----------------|---|-----------|---------|--------|----------|--------|----------|
|                |   |           | $k'$    | $k'_2$ | $\alpha$ | $k'_2$ | $\alpha$ |
| <b>P3-Me</b>   |    | 120       | 6.43    | 9.56   | 1.016    | 7.18   | 1.016    |
| <b>P3-Et</b>   |    | 120       | 9.31    | 13.49  | 1.000    | 10.22  | 1.013    |
| <b>P3-nPr</b>  |    | 120       | 15.67   | 23.15  | 1.000    | 17.02  | 1.010    |
| <b>P3-iPr</b>  |   | 120       | 10.84   | 15.63  | 1.000    | 11.55  | 1.011    |
| <b>P3-nBu</b>  |  | 120       | ND      | ND     | ND       | 28.47  | 1.009    |
| <b>P3-nPen</b> |  | 120       | ND      | ND     | ND       | 49.28  | 1.007    |
| <b>P4-Me</b>   |  | 120       | 5.28    | 6.93   | 1.024    | 5.38   | 1.000    |
| <b>P4-Et</b>   |  | 120       | 7.12    | 8.97   | 1.011    | 7.15   | 1.000    |
| <b>M6-Me</b>   |  | 120       | 6.01    | 9.68   | 1.038    | 6.55   | 1.000    |
| <b>M6-Et</b>   |  | 120       | 8.50    | 13.05  | 1.040    | 9.04   | 1.000    |
| <b>M15-Me</b>  |  | 120       | 0.55    | 1.06   | 1.030    | ND     | ND       |

| compound | structure   | temp.(°C) | OV-1701 | BSiMe           |       | BSiAc           |       |
|----------|---|-----------|---------|-----------------|-------|-----------------|-------|
|          |   |           | k'      | k' <sub>2</sub> | α     | k' <sub>2</sub> | α     |
| M16-Me   |    | 120       | 0.74    | 1.77            | 1.054 | ND              | ND    |
| M11-Me   |    | 120       | 0.47    | 0.87            | 1.156 | 0.93            | 1.077 |
| M11-Et   |    | 120       | 0.68    | 1.10            | 1.089 | 0.98            | 1.000 |
| M12-Me   |    | 120       | 0.29    | 0.49            | 1.078 | 0.74            | 1.295 |
| M12-Et   |    | 120       | 0.43    | 0.65            | 1.043 | 0.73            | 1.101 |
| M17-Me   |  | 120       | 0.23    | 0.52            | 1.088 | 0.72            | 1.087 |
| P2-Me    |  | 120       | 6.79    | 10.21           | 1.067 | 8.75            | 1.084 |
| P2-Et    |  | 120       | 9.15    | 13.10           | 1.039 | 10.55           | 1.048 |
| P13-Me   |  | 120       | 3.68    | 5.07            | 1.016 | 3.91            | 1.009 |
| P13-Et   |  | 120       | 4.99    | 6.56            | 1.000 | 5.15            | 1.000 |
| M9-Me    |  | 100       | 1.50    | 3.09            | 1.173 | 2.99            | 1.198 |
| M18-Me   |  | 100       | 0.37    | 0.58            | 1.039 | 0.415           | 1.000 |

| compound      | structure   | temp.(°C) | OV-1701 | BSiMe           |       | BSiAc           |       |
|---------------|---|-----------|---------|-----------------|-------|-----------------|-------|
|               |   |           | k'      | k' <sub>2</sub> | α     | k' <sub>2</sub> | α     |
| <b>C8-Me</b>  |    | 130       | 5.64    | 8.18            | 1.042 | 6.46            | 1.000 |
| <b>C8-Et</b>  |    | 130       | 7.57    | 10.35           | 1.015 | 8.39            | 1.000 |
| <b>M10-Me</b> |    | 130       | 8.68    | 13.01           | 1.113 | 9.94            | 1.009 |
| <b>M7-Me</b>  |    | 130       | 5.24    | 10.10           | 1.020 | ND              | ND    |
| <b>M7-Et</b>  |   | 130       | 6.81    | 12.30           | 1.036 | ND              | ND    |
| <b>M20-Me</b> |  | 130       | 5.24    | 6.55            | 1.029 | 6.00            | 1.028 |
| <b>M20-Et</b> |  | 130       | 6.95    | 8.44            | 1.036 | 7.46            | 1.011 |

#### Remarks

- Retention factors and separation factors shown in the table are representative values from only one run.
- k'<sub>2</sub> = retention factor of the second-eluted enantiomer
- ND = not determined
- Retention times of the same analyte under the same condition from two consecutive runs were within ± 0.003 minutes.
- Retention factors (k') were within ± 0.003 under the same condition and ± 0.008 on different day or different column length.
- Separation factors (α) were within ± 0.0005 in all cases.



### 4.3 Thermodynamic investigation by *van t Hoff* approach

In order to scrutinize the influence of analyte structure on the separation with cyclodextrin derivatives, thermodynamic parameters responsible for the analyte-stationary phase interaction and enantioselectivity of esters with similar structure were systematically investigated. Van't Hoff plots of  $\ln k'$  versus  $1/T$  for all series of esters on three columns were constructed. The relationships are all linear with the correlation coefficient ( $R^2$ ) greater than 0.998, with the exception of **M11-R**, **M12-R**, **M17-Me**, and **M9-Me** on BSiAc column. From these plots, enthalpy ( $\Delta H$ ) and entropy ( $\Delta S$ ) values were calculated. The relationships between  $\ln \alpha$  and  $1/T$  on two chiral columns were also plotted to obtain the  $\Delta(\Delta H)$  and  $\Delta(\Delta S)$  values. Theoretically, these plots should be linear; however, curvatures are observed for most analytes and would cause errors in the calculation of these parameters. Alternatively, the  $\Delta(\Delta H)$  and  $\Delta(\Delta S)$  values can also be calculated from the differences in  $\Delta H$  and  $\Delta S$  values of the two enantiomers; therefore, the  $\Delta(\Delta H)$  and  $\Delta(\Delta S)$  values in this study are obtained from the latter approach, instead.

In all cases, the  $-\Delta H_2$  and  $-\Delta S_2$  values on both chiral columns are higher than those on an achiral OV-1701 column. This would result from the increased interaction between analytes and cyclodextrin derivatives. Figures 4.4-4.5 show the differences in  $-\Delta H_2$  and  $-\Delta S_2$  values between chiral columns (BSiMe and BSiAc) and OV-1701 column.

According to figures 4.4-4.5, the increased interactions of **P3-R** (series 1) on BSiMe and BSiAc columns decrease with increasing alkyl chain. For alkyl esters of **P3**, longer alkyl chains increasingly interact with OV-1701 rather than cyclodextrin derivatives. Similarly, an increase in ester chain length of esters in series 2, 3, and 5 reduces the increased interaction strength and sites on two chiral columns relative to OV-1701 column. Interestingly, hydroxy-substituted esters (**M15-Me**, **M16-Me**, **M17-Me**, **M7-Me**, and **M7-Et**) possess relatively higher increased interactions on BSiMe column than any other esters in their series. This would be ascribed to the influence of hydroxy substituent, which is discussed later on the following sections.

For esters in series 3, **M11-R**, **M12-R**, and **M17-Me** show higher increased interactions on chiral columns than **P2-R** and **P13-R**, which exhibit rather low increased interaction relative to the overall interaction. This suggests that most of the interactions of **M11-R**, **M12-R**, and **M17-Me** on BSiMe and BSiAc columns result from the interaction between analytes and chiral phases. On the contrary, most of the interactions of **P2-R** and **P13-R** on chiral columns are due to the strong interactions between these esters and OV-1701 polysiloxane.

For esters in series 4, **M9-Me** exhibits substantially higher increased interactions on chiral columns relative to OV-1701 column than **P4-Me** and **M18-Me**. This shows that **P4-Me** and **M18-Me** strongly interact with achiral OV-1701 phase rather than with BSiMe and BSiAc phases.

Among all esters in series 5, the increased interactions of **M7-R** on BSiMe column are the highest. Similar to the observation of series 3, it could be assumed that hydroxy substituent strongly interacts with methoxy and acetoxy groups on BSiMe and BSiAc molecules, respectively.

Notably, esters with chloro, bromo, or hydroxy substituents in series 3 and 5 (**M11-Me**, **M12-Me**, **M17-Me**, and **M9-Me**), which can form polar interaction with acetoxy groups on BSiAc, exhibit higher increased interaction than any other ester analytes in all series.

ศูนย์วิทยทรัพยากร  
จุฬาลงกรณ์มหาวิทยาลัย

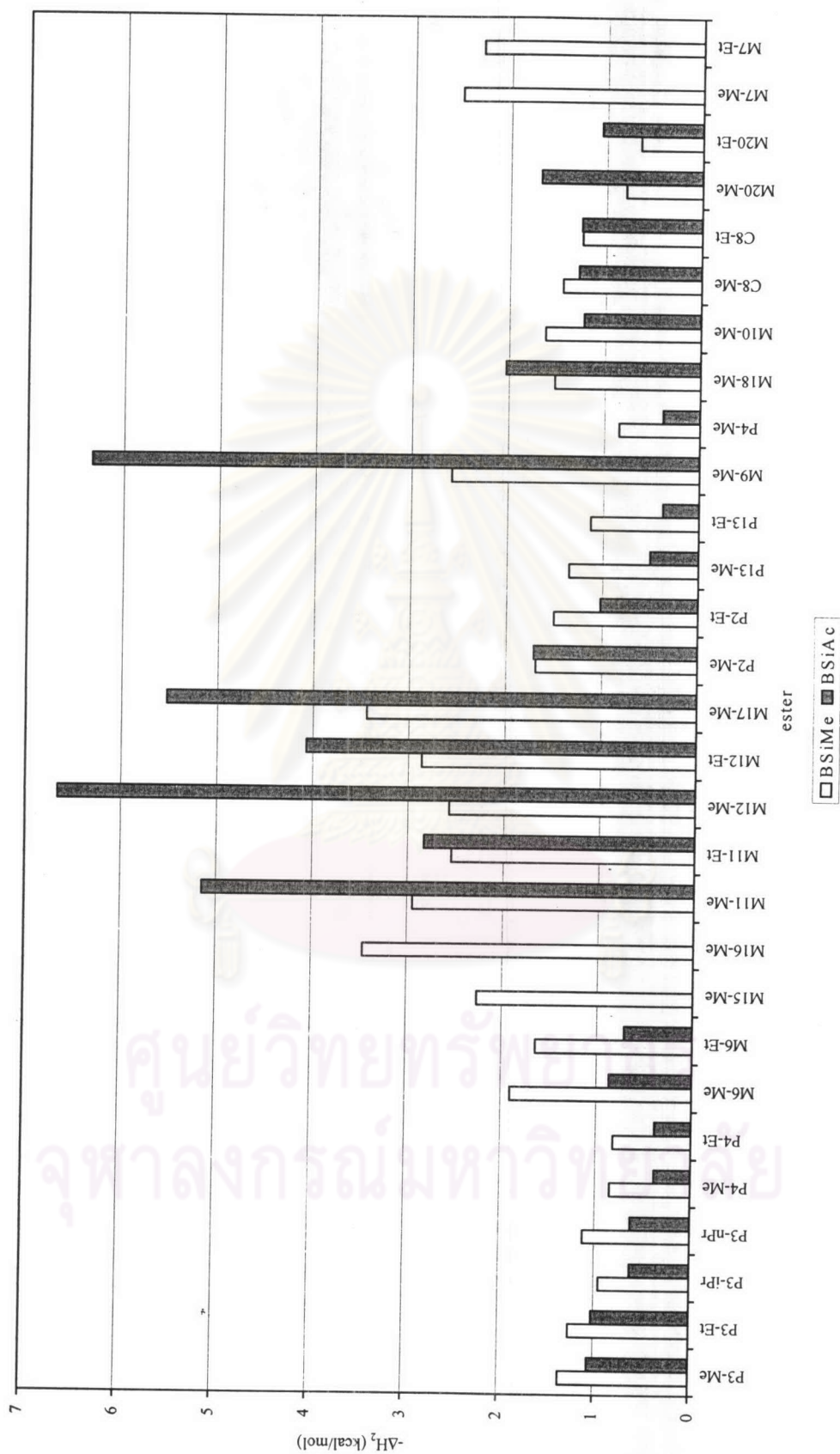


Figure 4.4 Differences in  $-\Delta H_2$  values for second-eluted enantiomers of esters (series 1-5) between chiral columns and OV-1701 column



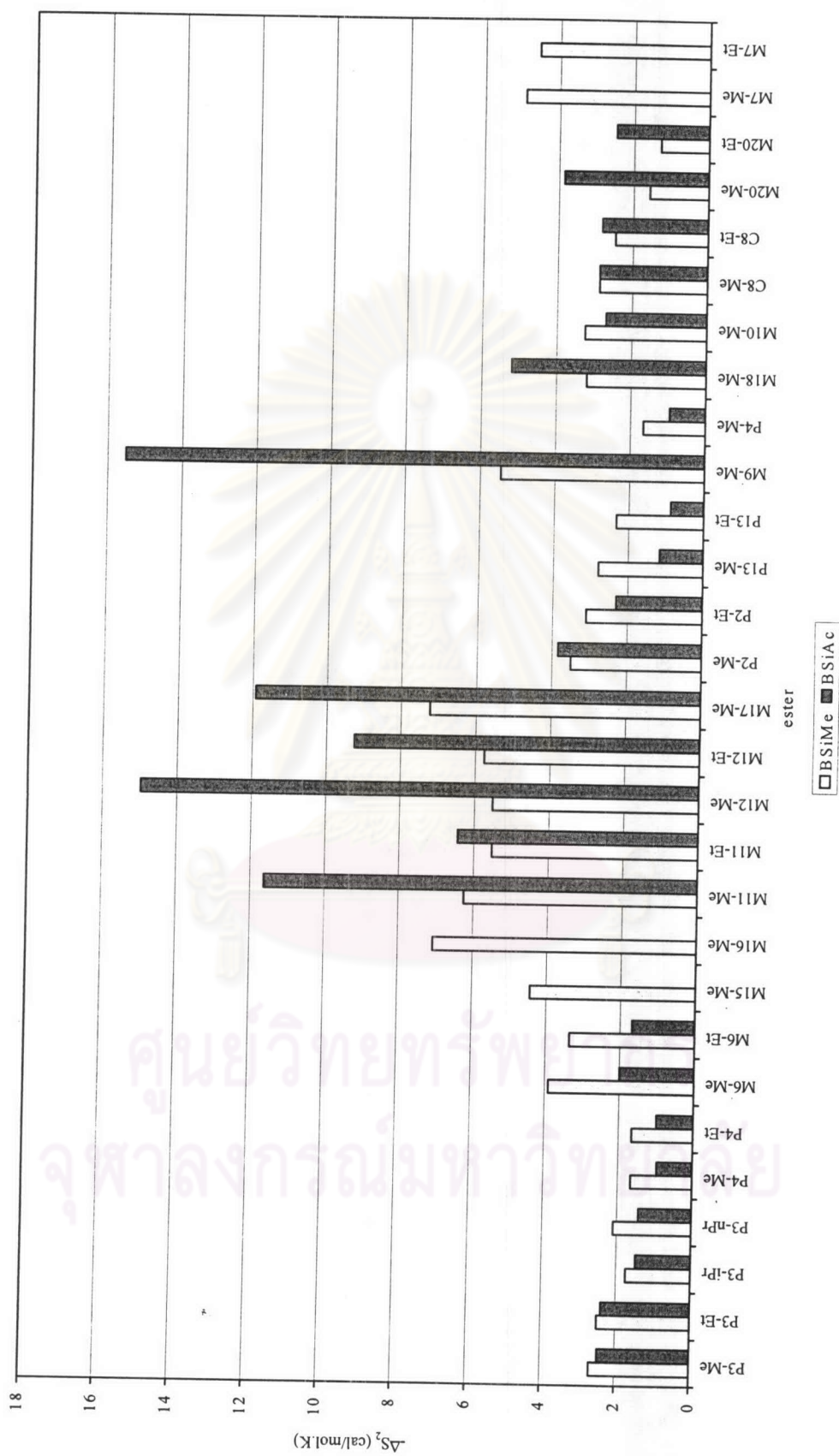
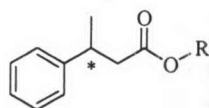


Figure 4.5 Differences in  $-\Delta S_2$  values for second-eluted enantiomers of esters (series 1-5) between chiral columns and OV-1701 column

#### 4.3.1 Esters with different alkyl chain length (Series 1)



**P3-R**  
alkyl esters of 3-phenylbutyric acid

Esters in series 1 are composed of alkyl esters of 3-phenylbutyric acid (or **P3-R**) with methyl, ethyl, *n*-propyl, isopropyl, *n*-butyl, or *n*-pentyl as the alkyl groups. Thermodynamic data for the separation of these esters on BSiMe and BSiAc columns are illustrated in figures 4.6-4.9.

As shown in figures 4.6-4.7, the strength of interaction and the number of interaction sites of this homologous series towards these stationary phases slightly increase with lengthening alkyl chain (higher values of overall  $-\Delta H$  and  $-\Delta S$ ). However, this is opposite to the trends observed from figures 4.4-4.5, in which the increased interactions decrease with lengthening alkyl chain. This would mean that most of the interactions on chiral phases result from additional interaction between analytes and non-chiral polysiloxane. For isomeric alkyl esters, the interaction of straight alkyl chain ( $R = n$ -propyl) is greater than that of branched alkyl chain ( $R =$  isopropyl). Comparing the  $-\Delta H$  and  $-\Delta S$  values on two chiral phases, the degrees of interaction strength and interaction sites of these esters on BSiMe column are slightly higher than on BSiAc column.

However, enantioselectivity of BSiAc phase for all esters are greater than that of BSiMe phase, according to figures 4.8-4.9. All enantiomers of **P3-R** could be separated on BSiAc column while only methyl ester could be resolved on BSiMe column. Nevertheless, the discrimination between individual enantiomers clearly decreases with increasing ester chain length. Besides, branched alkyl ester shows better enantioseparation than straight alkyl ester, opposite to the trend in  $-\Delta H$  and  $-\Delta S$  values. Figure 4.10 shows the comparison of the separation of **P3-Me** on both chiral columns at 110 °C, indicating the slightly superior enantioselectivity of BSiAc phase in shorter analysis time. This is not in agreement with the thermodynamic result, which shows that the enantioselectivity of **P3-Me** BSiAc phase is twice higher than that on BSiMe phase. Considering the  $\ln \alpha$  vs.  $1/T$  plot (figure 4.11),  $\alpha$  values on BSiAc phase increase more rapidly with decreasing temperature than those on BSiMe

phase. Thus, chromatographic separation data at only a given temperature cannot provide complete information about enantioseparation. It should be considered from thermodynamic data instead.

Similar results of the influence of ester chain length on chiral separation were obtained by Jaques et al. [12]. It was observed that increasing the ester chain length decreased enantioselectivity of analytes separated on 2,3-di-*O*-acetyl-6-*O*-*tert*-butyldimethylsilyl- $\beta$ -cyclodextrin. Jaques proposed that the loss of selectivity resulted from an increase in the apolar character of ester function in the polar cyclodextrin medium. This was probably due to the small  $\beta$ -cyclodextrin ring which forced the alkyl chain into interacting unfavorably with the polar C2-3 rim unavoidably.

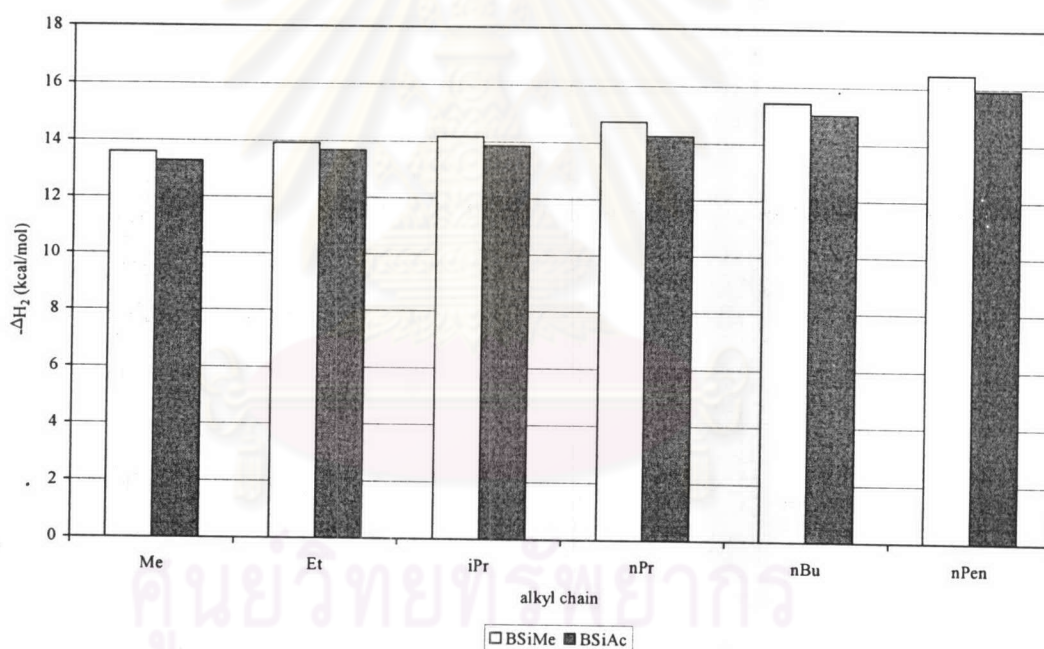


Figure 4.6 Enthalpy values for second-eluted enantiomers of esters (series 1) on BSiMe and BSiAc columns



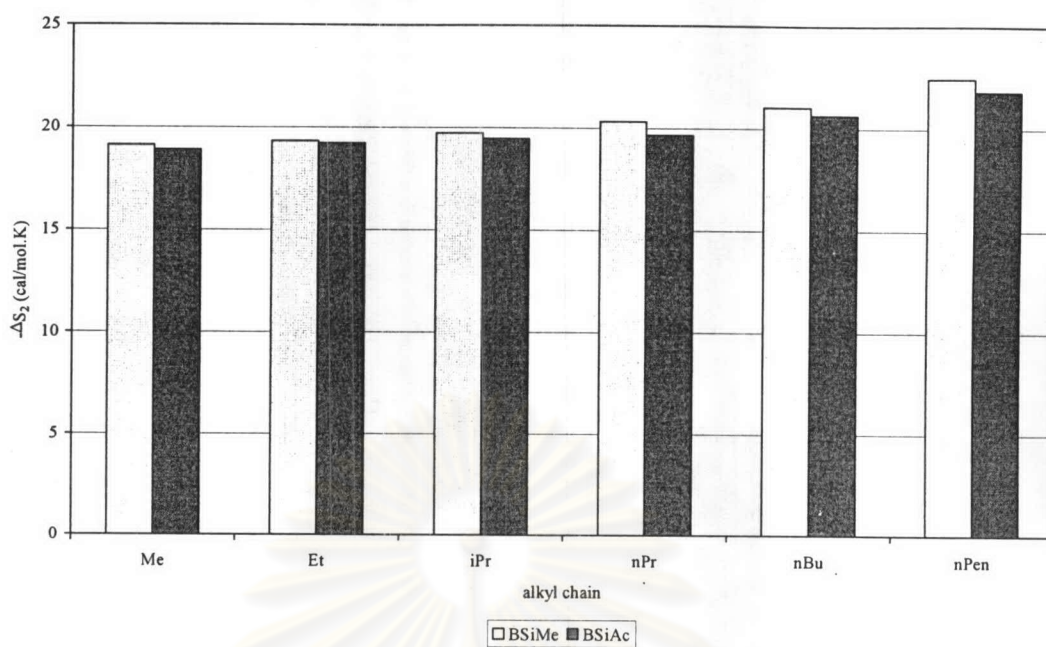


Figure 4.7 Entropy values for second-eluted enantiomers of esters (series 1) on BSiMe and BSiAc columns

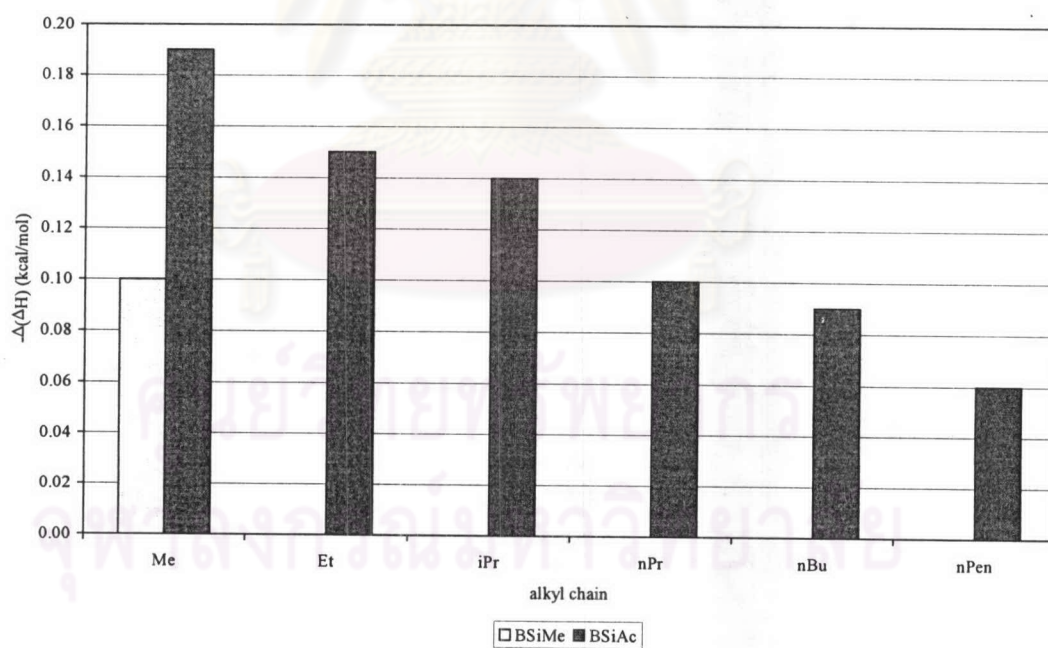


Figure 4.8 Differences in enthalpy values for enantiomers of esters (series 1) on BSiMe and BSiAc columns

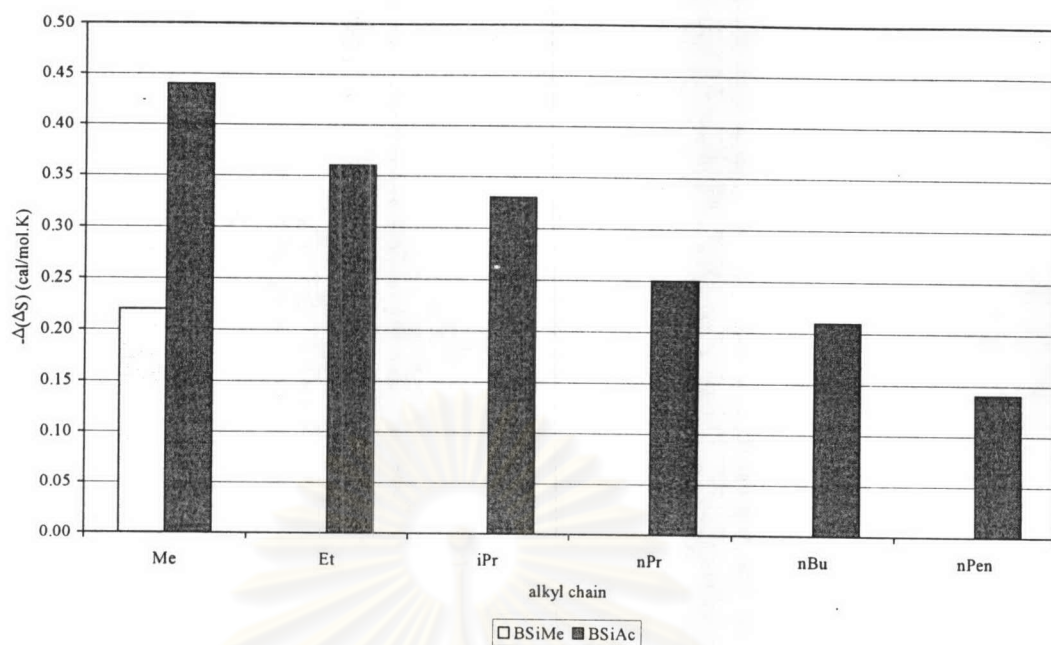


Figure 4.9 Differences in entropy values for enantiomers of esters (series 1) on BSiMe and BSiAc columns

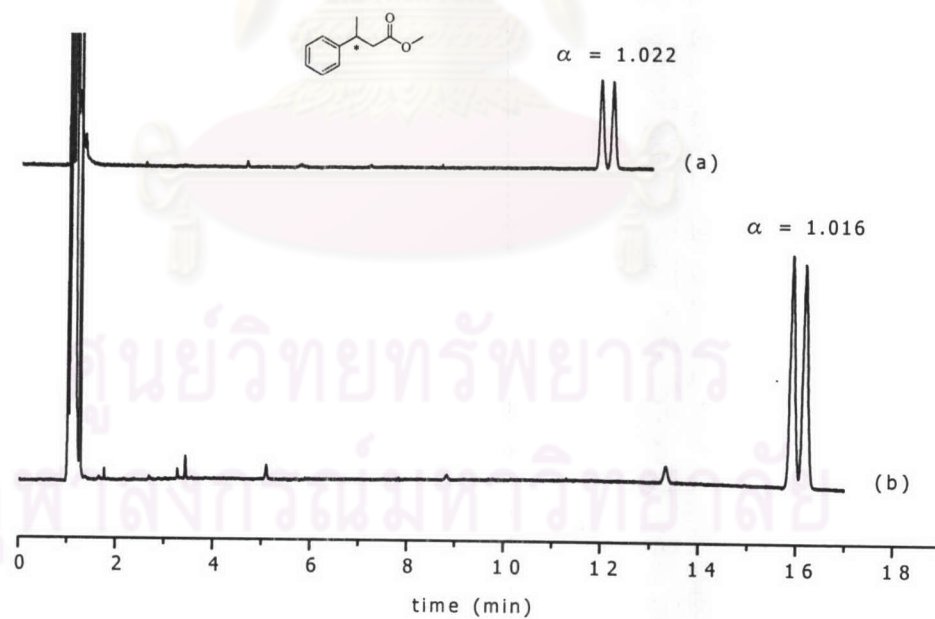


Figure 4.10 Separation of P3-Me at 110 °C on (a) BSiAc and (b) BSiMe columns

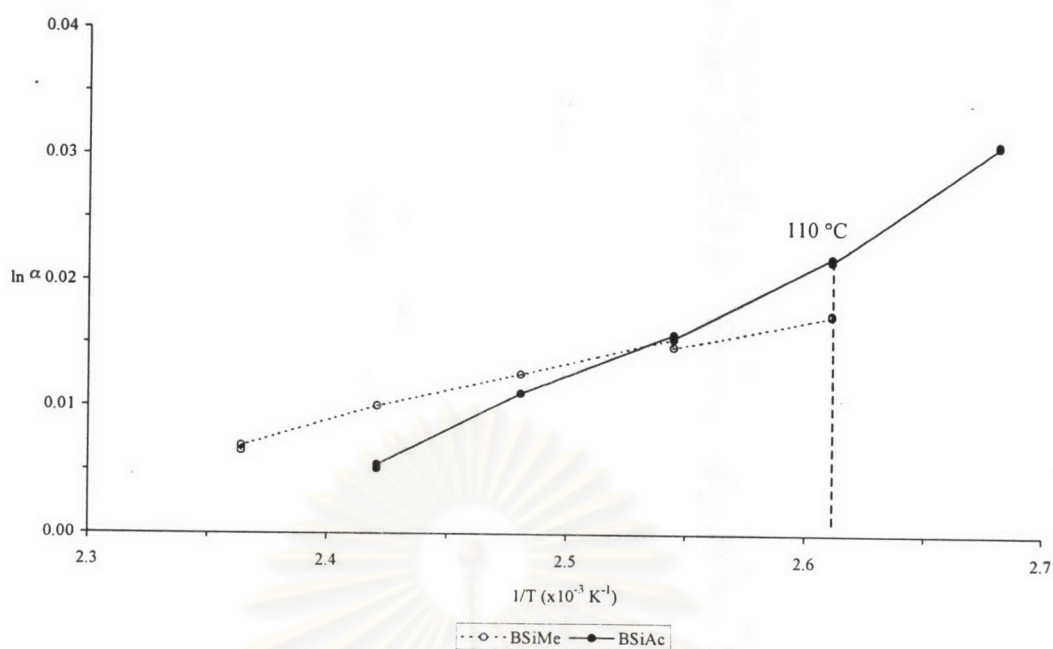
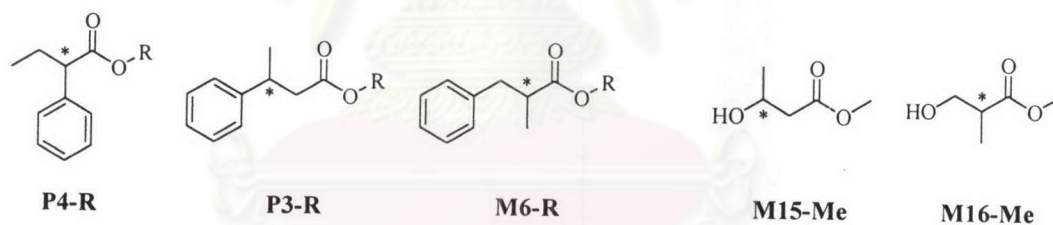


Figure 4.11 plots of  $\ln \alpha$  versus  $1/T$  of **P3-Me** on BSiMe and BSiAc columns

#### 4.3.2 Esters with different positions of substituent or chiral center (Series 2)



Analytes in series 2 are divided into two subgroups of positional isomers: subgroup I consists of **P4-R**, **P3-R**, and **M6-R**; subgroup II consists of **M15-Me**, **M16-Me**. Owing to peak tailing effect, the separation data of **M15-Me** and **M16-Me** on BSiAc column are unavailable. Thermodynamic parameters responsible for the separation of these esters are presented in figures 4.12 – 4.15.



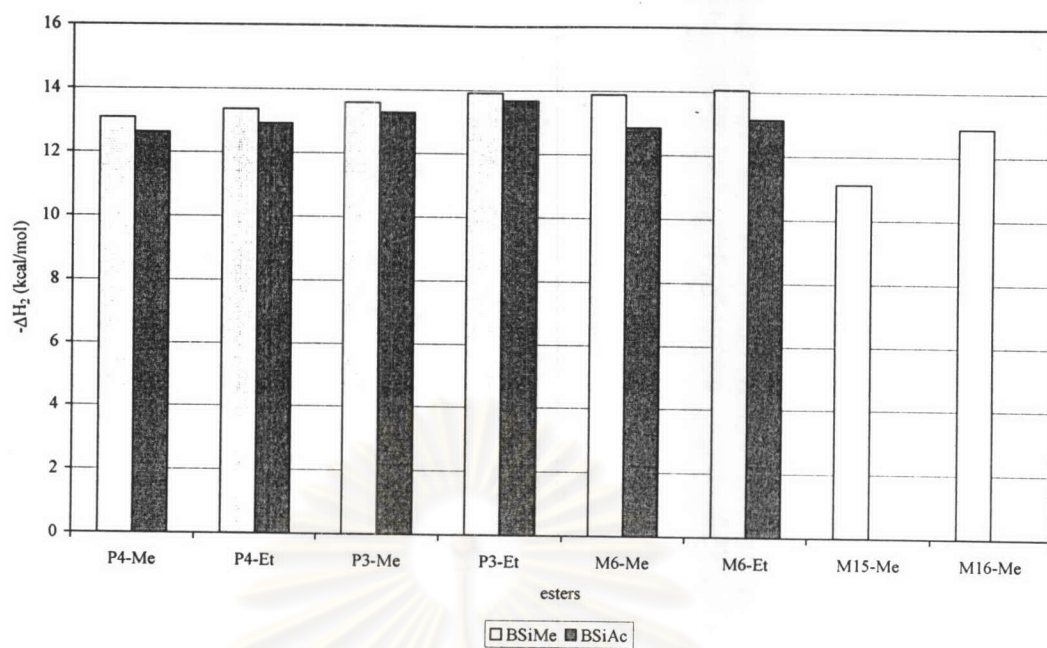


Figure 4.12 Enthalpy values for second-eluted enantiomers of esters (series 2) on BSiMe and BSiAc columns

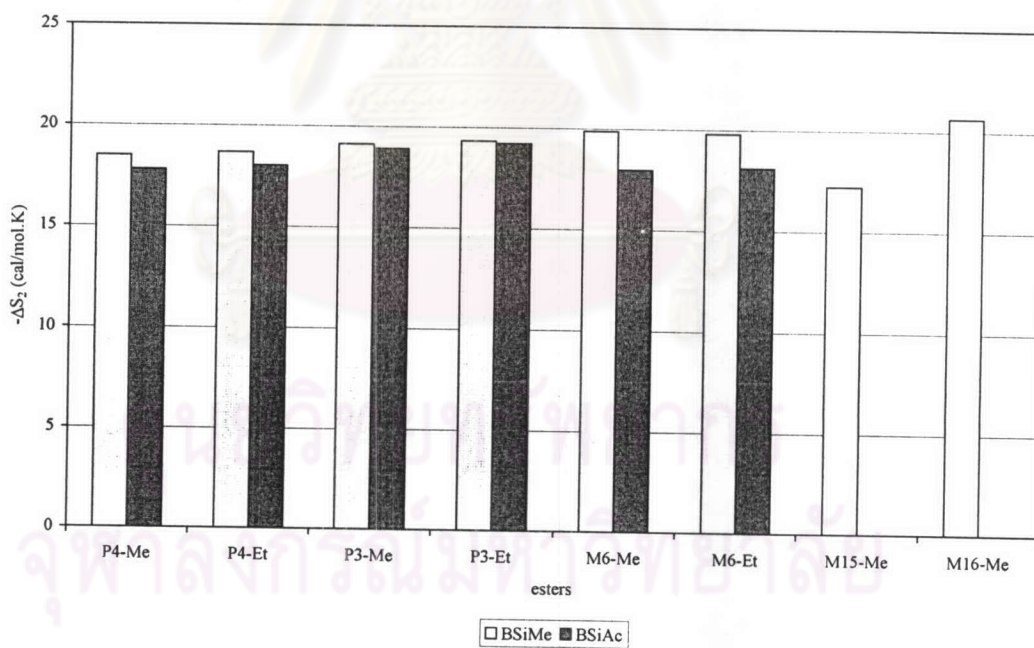


Figure 4.13 Entropy values for second-eluted enantiomers of esters (series 2) on BSiMe and BSiAc columns

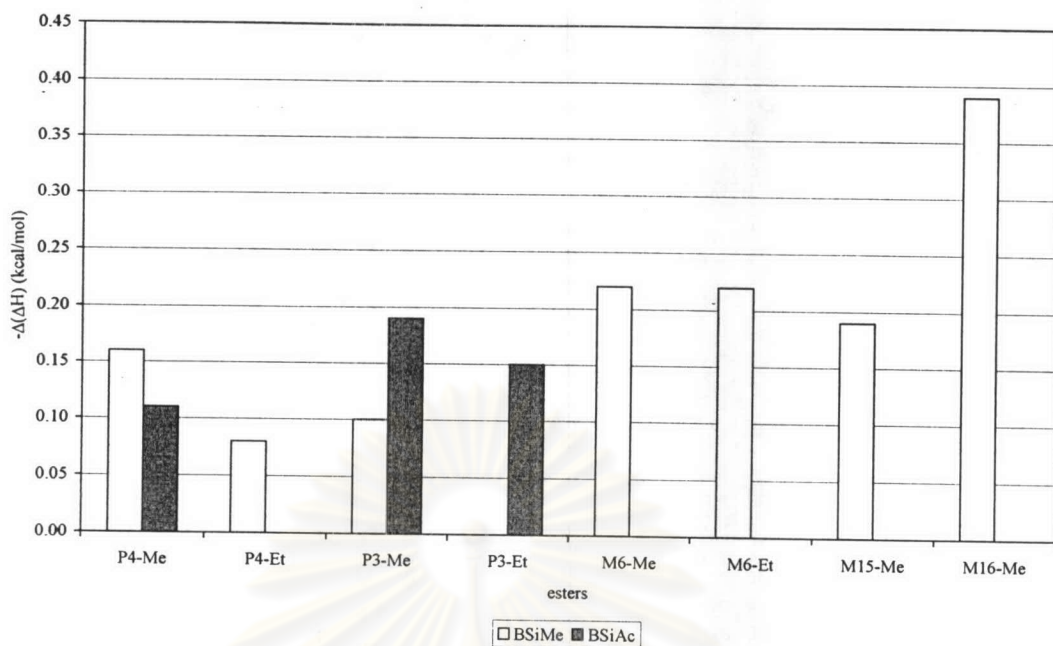


Figure 4.14 Differences in enthalpy values for enantiomers of esters (series 2) on BSiMe and BSiAc columns

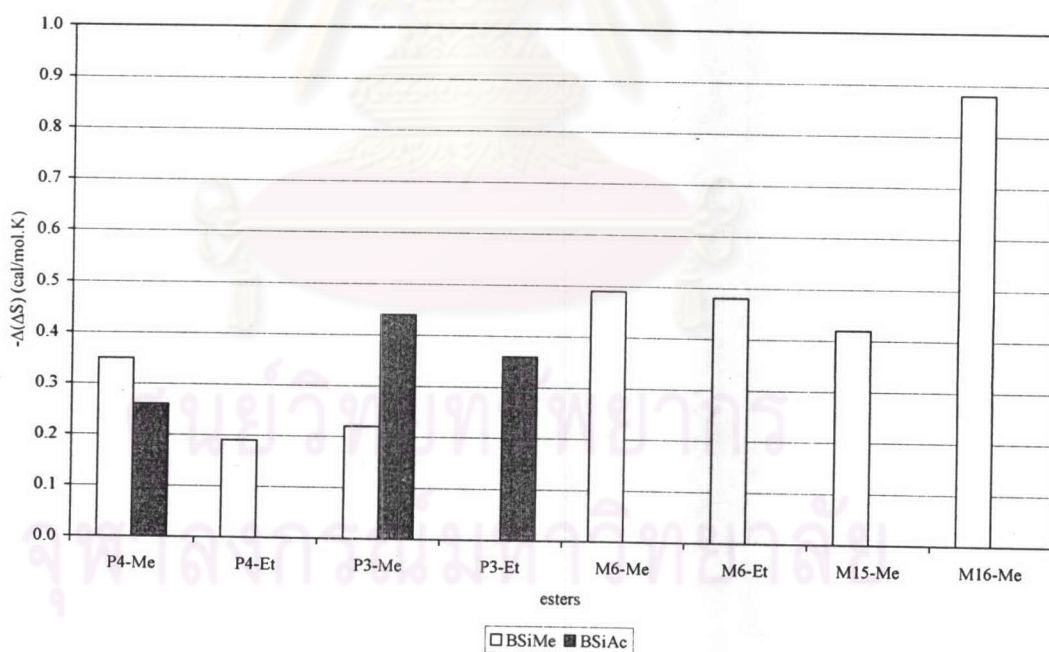
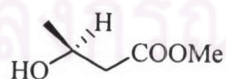
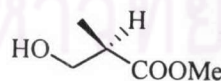


Figure 4.15 Differences in entropy values for enantiomers of esters (series 2) on BSiMe and BSiAc columns

The thermodynamic parameters of methyl and ethyl derivatives of esters (subgroup I) on both chiral columns show similar trend as those in series 1, in which longer alkyl group (ethyl) slightly increases the retention but decreases or has no influence on the enantioseparation. On BSiMe column, isomers of methyl esters in subgroup I exhibited similar interaction ( $-\Delta H$  and  $-\Delta S$ ) towards the stationary phase, with a slight increase from **P4-Me** < **P3-Me** < **M6-Me**. However, the discrimination between individual enantiomers showed a different trend: **P3-Me** < **P4-Me** < **M6-Me**. This indicates that the enantioseparation decreases with the increased distance of chiral center away from the carboxyl group. Interestingly, longer ethyl chain of **M6-R**, with the highest separation among three isomers, showed no influence on the chiral resolution, i.e. similar  $-\Delta(\Delta H)$  and  $-\Delta(\Delta S)$  values for **M6-Me** and **M6-Et**.

For esters in subgroup II on BSiMe column, **M16-Me**, with the chiral center near the carboxyl group, displayed the strongest interaction and highest enantioseparation. Furthermore, *R* and *S* configurations of enantiomers of **M15-Me** and **M16-Me** were assigned with enantiomerically pure standards. It was observed that the interaction between *S*-enantiomer of **M15-Me** and BSiMe phase is weaker than that of *R*-enantiomer (*S* eluted before *R*). The contrary result was obtained for the separation of **M16-Me**, *R* eluted before *S*. However, considering configuration of chiral carbon atoms by using Cahn-Ingold-Prelog convention, it was observed that spatial arrangement of both *S*-enantiomer of **M15-Me** and *R*-enantiomer of **M16-Me** are the same. Therefore, it is necessary to consider not only the configuration assignment (*R* or *S*) but also the spatial arrangement of atom or group bonded to chiral center.

**(S)-M15-Me****(R)-M16-Me**

Considering the similar pattern of the substitution between these two subgroups (**P3-Me**, **M6-Me** vs. **M15-Me**, **M16-Me**) on BSiMe column, it is surprising to observe that  $-\Delta(\Delta H)$  and  $-\Delta(\Delta S)$  values of  $\alpha$ -methyl esters (**M6-Me** and **M16-Me**) are twice the values of  $\beta$ -methyl esters (**P3-Me** and **M15-Me**). This



observation clearly shows the dependence of the enantioselectivity on the position of substituent. When comparing two types of substituent, phenyl (**P3-Me**, **M6-Me**) and hydroxyl (**M15-Me**, **M16-Me**), the phenyl-substituted enantiomers showed relatively higher interaction, except for the  $-\Delta S$  value of **M16-Me**. Nonetheless, the hydroxyl-substituted analytes exhibited better separation than their phenyl analogues.

As proposed by Beier and Holtje [43], who studied enantioselective binding properties of BSiMe, the main contribution to enantiomer separation results from inclusion effects. Moreover, hydrogen bonds are helpful to stabilize the intermediate diastereomeric complexes in the case of hydroxyl-substituted analytes. These explanations could be applied to our results in this group of analytes. Possibly, greater enantioselectivity of hydroxyl-substituted esters is due to hydrogen bonds between hydroxyl of esters and ether oxygen atoms of BSiMe. According to Beier and Holtje, although hydrogen bonds are not necessary for chiral separation, the stabilizing effect of hydrogen bonds is useful to form strong contacts with the chiral centers at C2 and C3 wider opening of the cyclodextrin cavity and to cause an orientation favorable to chiral recognition. This is apparently observable from higher  $-\Delta S$  values of **M16-Me**, with hydroxyl at chiral center, than those of **M6-Me**. Besides, phenyl-substituted esters are likely too steric to fit deeply and tightly into the cavity of the modified cyclodextrin.

Although different isomers of esters subgroup I showed similar interaction towards BSiAc and BSiMe columns, their separations on BSiAc column are totally different from those on BSiMe column (figures 4.16-4.17). While **M6-Me** gave the best separation on BSiMe column, it was not separable at all on BSiAc column. **P3-Me** showed the smallest separation among the methyl derivative of three isomers on BSiMe column; however, it exhibited the largest separation on BSiAc column. This would be the influence of not only the position of substituent or chiral center on ester but also the substitution at the chiral C-2 and C-3 positions of cyclodextrin.

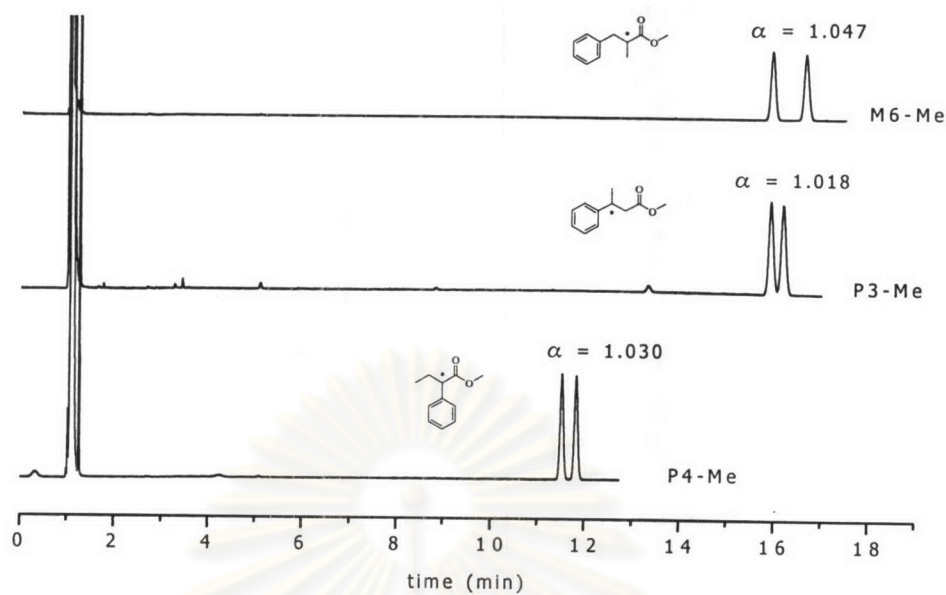


Figure 4.16 Separation of esters in series 2 (subgroup I) at 110 °C on BSiMe column

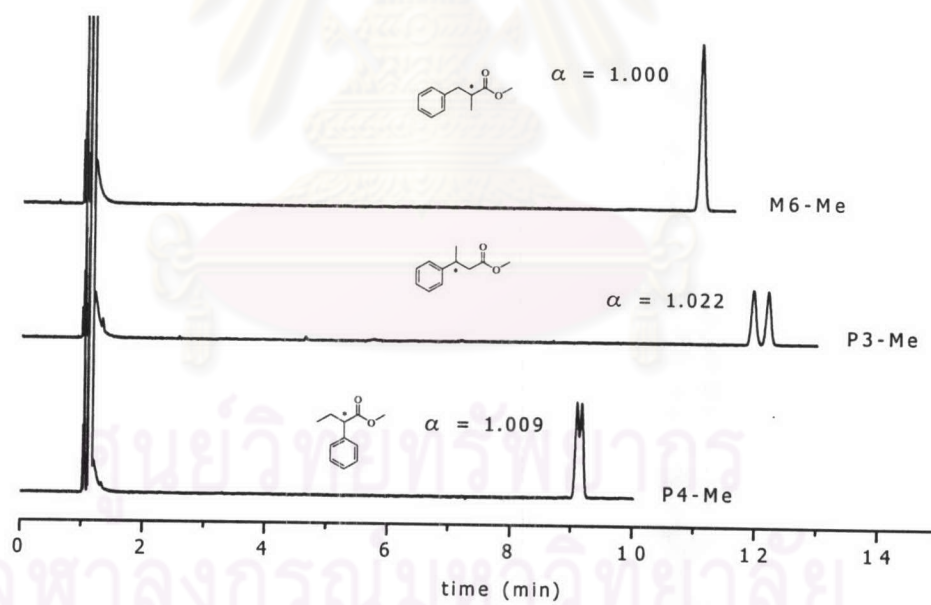
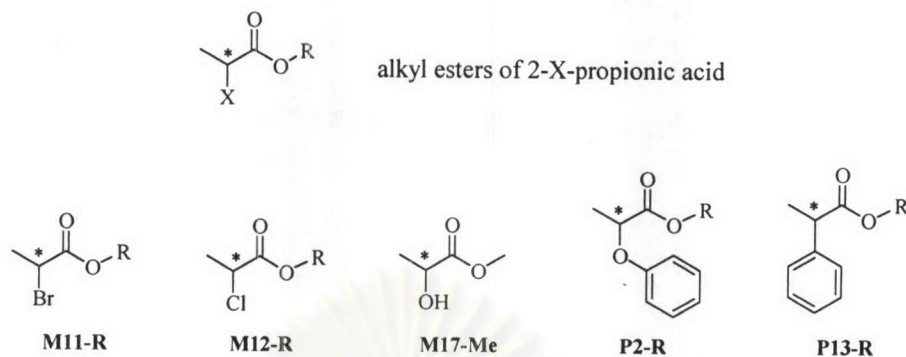


Figure 4.17 Separation of esters in series 2 (subgroup I) at 110 °C on BSiAc column

### 4.3.3 Esters with different types of substituents, alkyl esters of 2-X-propionic acid (Series 3)



This series incorporates methyl and ethyl esters of 2-X-propionic acid (X = Cl, Br, OH, Ph, OPh). Within this group of esters, the effect of substituent at 2-position and alkyl chain length can be studied. Thermodynamic data responsible for the interaction and discrimination of analytes in this group are depicted in figures 4.18-4.21.

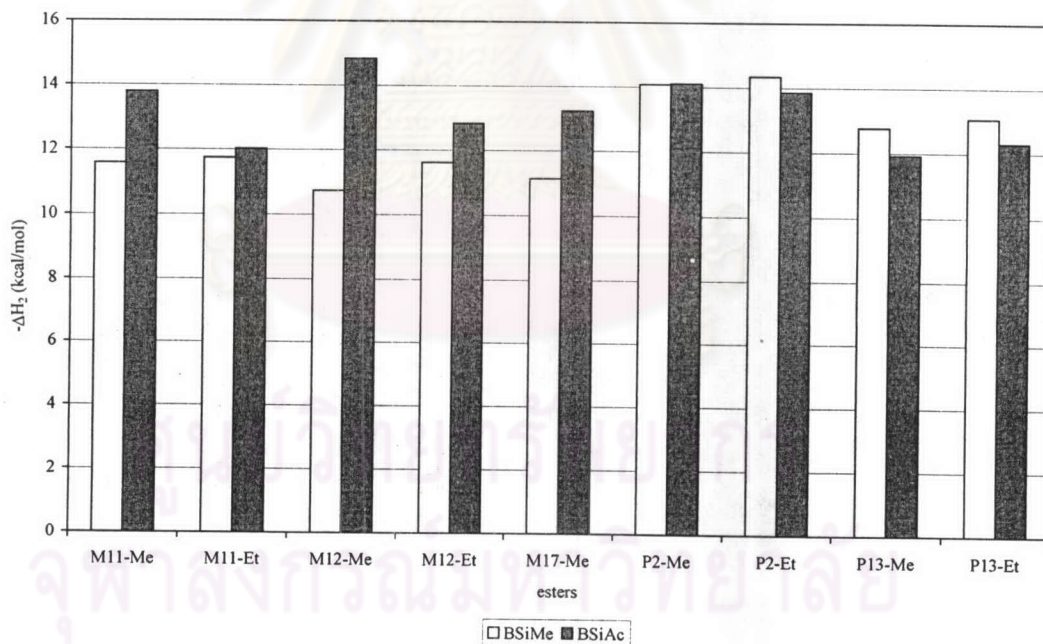


Figure 4.18 Enthalpy values for second-eluted enantiomers of esters (series 3) on BSiMe and BSiAc columns



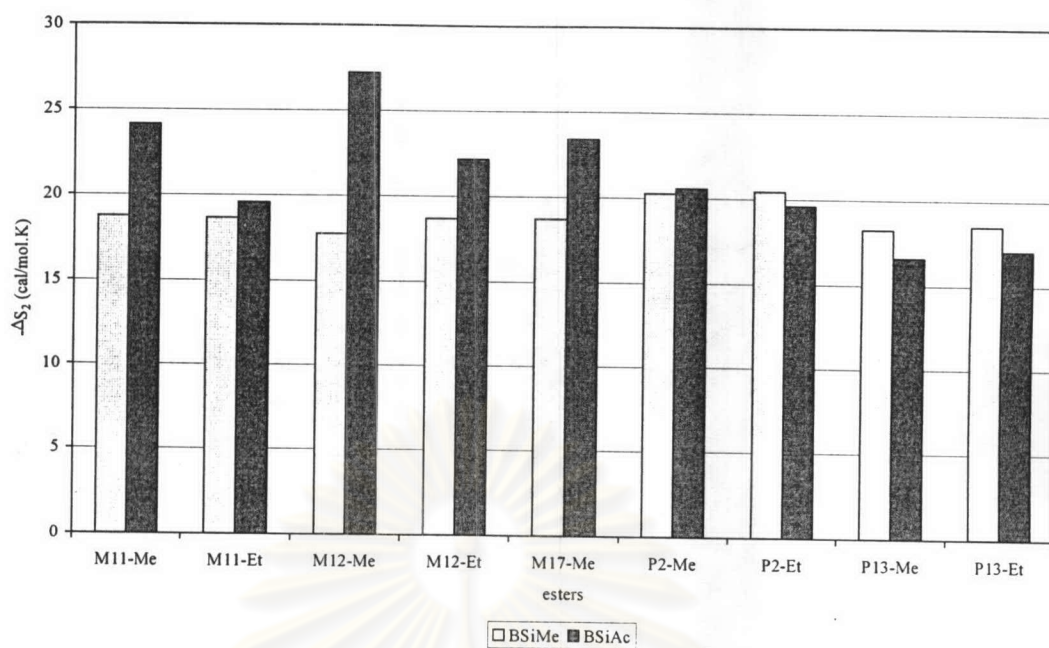


Figure 4.19 Entropy values for second-eluted enantiomers of esters (series 3) on BSiMe and BSiAc columns

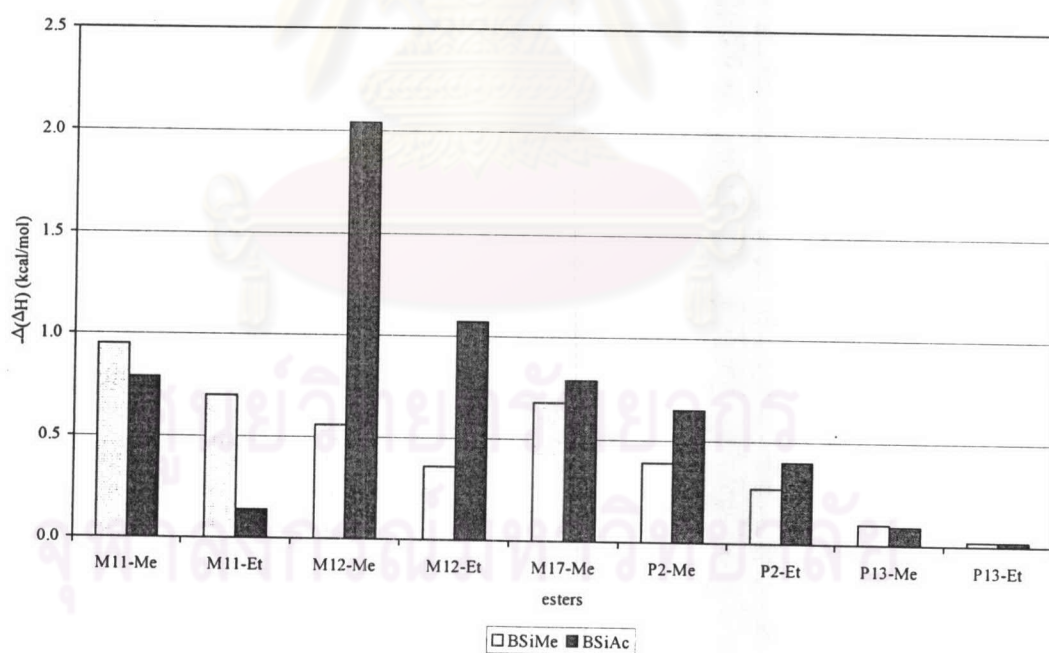


Figure 4.20 Differences in enthalpy values for enantiomers of esters (series 3) on BSiMe and BSiAc columns

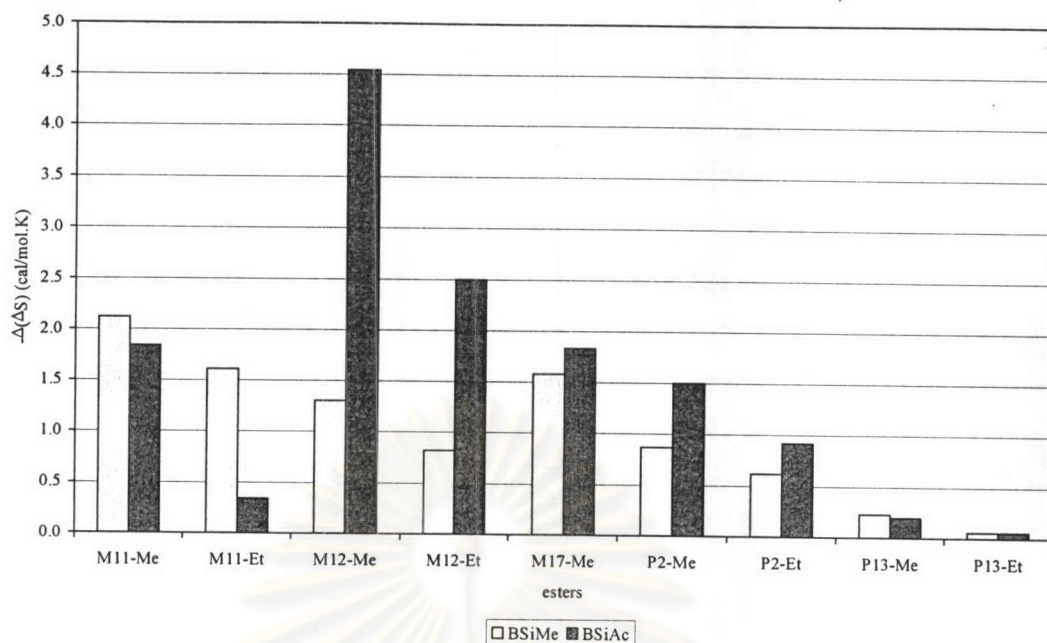


Figure 4.21 Differences in entropy values for enantiomers of esters (series 3) on BSiMe and BSiAc columns

Similar to the preceding sections, it is observed that changing alkyl group from methyl to ethyl generally results in a slight increase in the interaction of this group of esters towards BSiMe phase. However, the chiral recognition of enantiomers decreases dramatically. The  $-\Delta H$  and  $-\Delta S$  values of all esters on the BSiMe column are not much different from each other regarding the type of substituent, except for **P2-R** which has relatively higher  $-\Delta H$  and  $-\Delta S$  values. Nevertheless, types of substituent impact enantioselectivity significantly. Changing the halogen substituent from chloro to bromo causes the  $-\Delta(\Delta H)$  and  $-\Delta(\Delta S)$  values to increase considerably (approximately two times), which suggests that the resolution of ester analytes increases with increasing the size of substituent. Considering **M12-Me** (chloro-substituted) and **M17-Me** (hydroxyl-substituted), the trend is not in agreement with the aforementioned assumption that an increase in substituent size improves enantioselectivity. **M17-Me** has slightly higher  $-\Delta(\Delta H)$  and  $-\Delta(\Delta S)$  values than those of **M12-Me**, probably due to hydrogen bonding between hydroxyl group of **M17-Me** and methoxy groups at C-2 and C-3 on BSiMe molecule. In this case, the size of substituent is not the primary contribution to chiral separation. Instead, hydrogen bonds dominate enantioselectivity. The influence of polar interaction was observable from the chiral separation of **P2-R** and **P13-R** as well. Phenoxy group of



**P2-R** can form additional dipole interaction with methoxy groups on the cyclodextrin ring; therefore, **P2-R** exhibits better separation than **P13-R**. Noticeably, enantioselectivity of hydroxyl-substituted ester was superior to that of phenyl-substituted esters, similar to the results obtained from esters in series 2.

Contrary to the results obtained from BSiMe phase, changing alkyl ester from methyl to ethyl substantially reduces the interaction between analytes and BSiAc phase as well as the chiral recognition of enantiomers of esters, except for **P13-R**. Moreover, the interactions of **M12-Me**, **M11-Me**, and **M17-Me** towards BSiAc phase are much higher than their interactions towards BSiMe phase. Unlike the separation on BSiMe column, substituent type pronouncedly affects the interaction strength and sites of compounds towards BSiAc phase. With this phase, chloro-substituted **M12-Me** showed the strongest interaction and largest  $-\Delta(\Delta H)$  and  $-\Delta(\Delta S)$  values among all analytes. Opposite to the results obtained on BSiMe phase, the enantioselectivity extremely deteriorated as the size of halogen substituent increased. This would be assumed that the size of substituent is the crucial contribution to the separation. However, the substituent size is not the only factor determining the enantioseparation in this case because the small hydroxyl group of **M17-Me** did not exhibit as large separation as the chloro-substituted **M12-Me**. Therefore, it should be the combination of several contributions, e.g. hydrogen bond and dipole-dipole interaction, that lead to such a large separation.

Moreover, *R* and *S* configurations of **M12-Me** and **M17-Me** enantiomers were assigned with enantiomerically pure standards. It is interesting to observe that, on BSiMe column, *S*-enantiomer of **M12-Me** eluted before *R*-enantiomer while **M17-Me** eluted with the opposite order, *R* prior to *S*. However, on BSiAc column *R*-enantiomers of both **M12-Me** and **M17-Me** eluted before *S*-enantiomers.

Comparing BSiMe phase with BSiAc phase, enantioseparation of ester analytes on two chiral columns was very different (figures 4.22-4.23), possibly due to the difference in substitution at C-2 and C-3 of CD molecule. Opposite to the results on BSiMe phase, enantioselectivities of ester analytes on BSiAc substantially decrease with an increase in not only ester chain length but also the size of halogen substituent. These likely result from the steric effect of acetoxy



groups, leading to narrower opening at the secondary face, which may impede the inclusion of analytes into the cyclodextrin cavity. In general, the chiral recognition ability of BSiAc phase for this group of esters was superior to that of BSiMe phase. Enantioselectivities of 2-chloro, 2-hydroxy, and 2-phenoxy substituted esters were greater on BSiAc than on BSiMe phase while those of 2-bromo and 2-phenyl substituted esters on two columns were very similar. In addition to the size effect, these differences can be ascribed to polar interactions between acetoxy on cyclodextrin and hydroxyl or phenoxy on esters.

Some ester analytes in this series (**M11-R** and **M12-R**) were formerly studied by Venema [7], using perpentyl  $\beta$ -cyclodextrin as a chiral stationary phase. Similar results to our studies on BSiMe column were obtained: changing alkyl chain from methyl to ethyl or changing halogen from bromo to chloro caused the loss of enantioselectivities. It was explained that longer alkyl chain likely hindered the accommodation of analyte molecules into the cyclodextrin cavity.

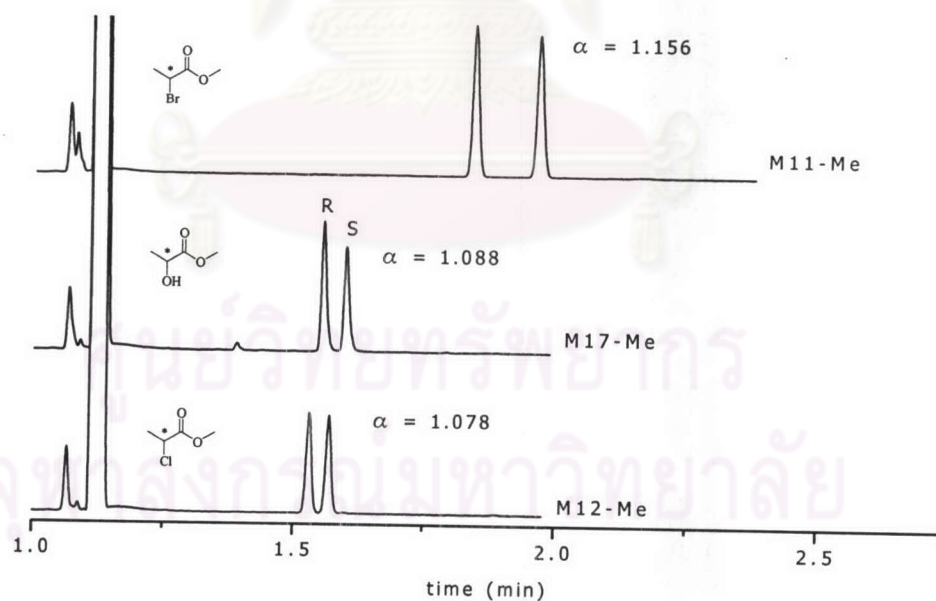


Figure 4.22 Separation of esters in series 3 at 120 °C on BSiMe column (**M17-Me** was prepared with *R*-enantiomer enriched.)

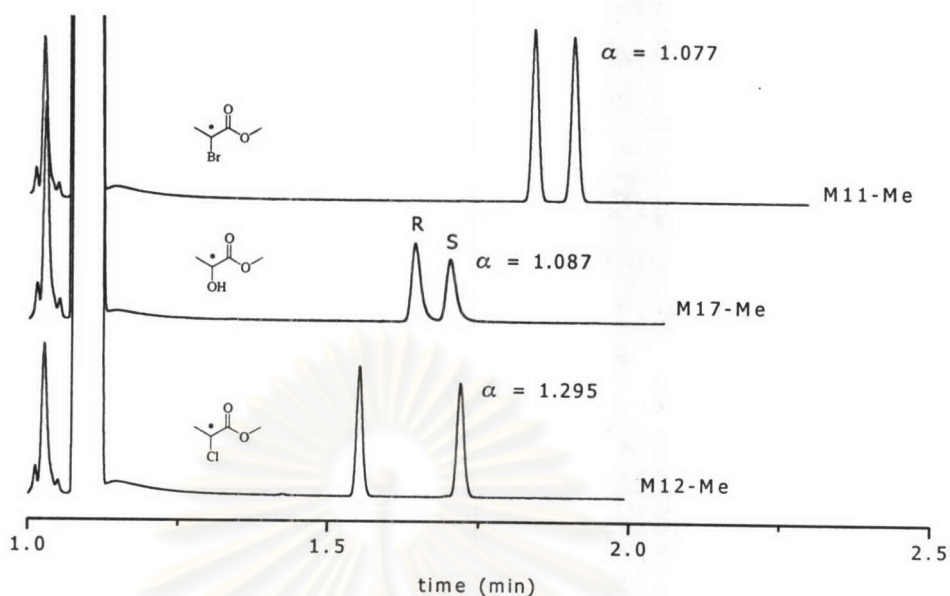
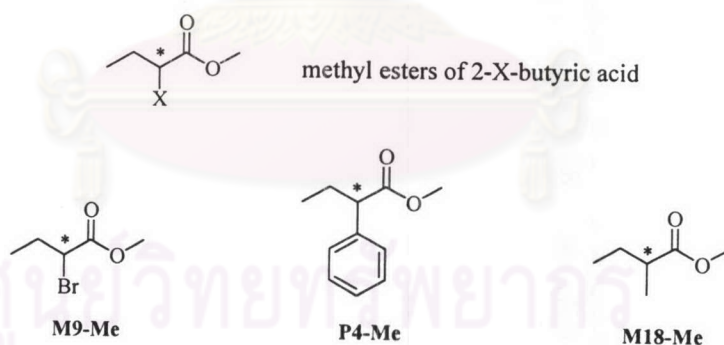


Figure 4.23 Separation of esters in series 3 at 120 °C on BSiAc column (**M17-Me** was prepared with *R*-enantiomer enriched.)

#### 4.3.4 Esters with different types of substituents, methyl esters of 2-*X*-butyric acid (Series 4)



This series includes methyl esters of 2-*X*-butyric acid (*X* = Ph, Br, Me). Within this group of esters, the effect of substituent at 2-position of butyric acid can be studied. The enthalpy and entropy results obtained for the separation of enantiomers are presented in figures 4.24 – 4.27.

The trend of the  $-\Delta(\Delta H)$  and  $-\Delta(\Delta S)$  values on both BSiMe and BSiAc phases are very similar to those of series 3: bromo-substituted **M9-Me** showed

higher selectivity than less polar phenyl-substituted **P4-Me** and methyl-substituted **M18-Me**.

Of all analytes in this group, **M9-Me** exhibits the highest  $-\Delta(\Delta H)$  and  $-\Delta(\Delta S)$  values on the two chiral columns. This can be probably ascribed to the polarizability of bromo substituent ( $\mu_{C-Br} = 1.82$ ,  $\mu_{C-CH_3} = 0.0$ , where  $\mu$  = group dipole moment in debye [44]) which causes additional weak dipole interaction with methoxy groups on BSiMe phase. Similarly, **M9-Me** possesses highest interaction strength and sites together with enantioselectivity among the three esters on BSiAc column, which is greater than those on BSiMe column, possibly due to stronger dipole interaction with acetoxy groups of cyclodextrin.

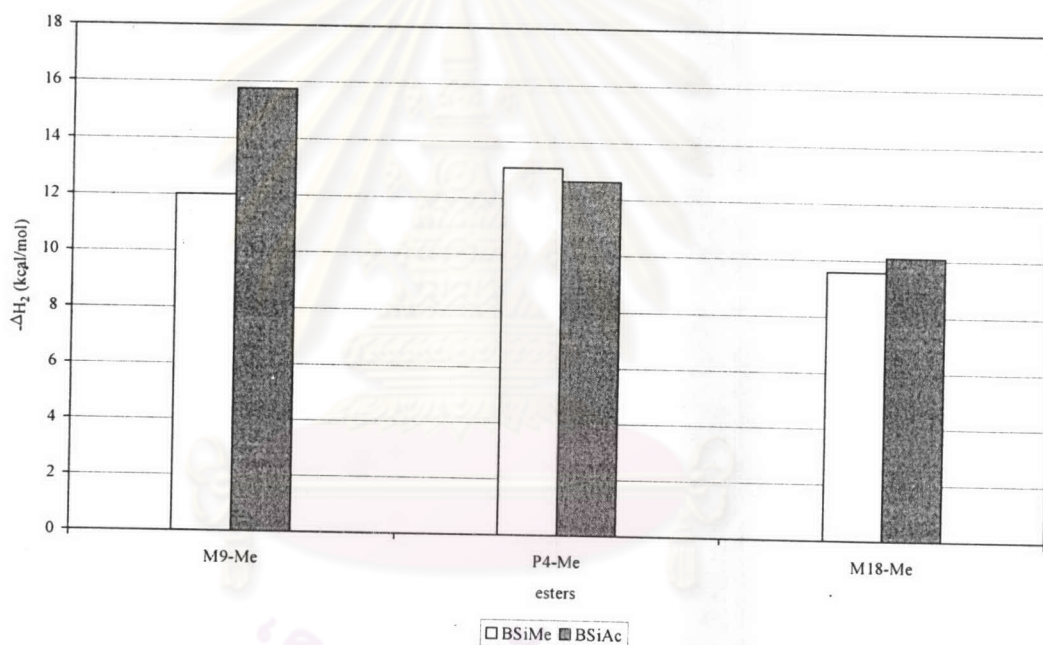


Figure 4.24 Enthalpy values for second-eluted enantiomers of esters (series 4) on BSiMe and BSiAc columns



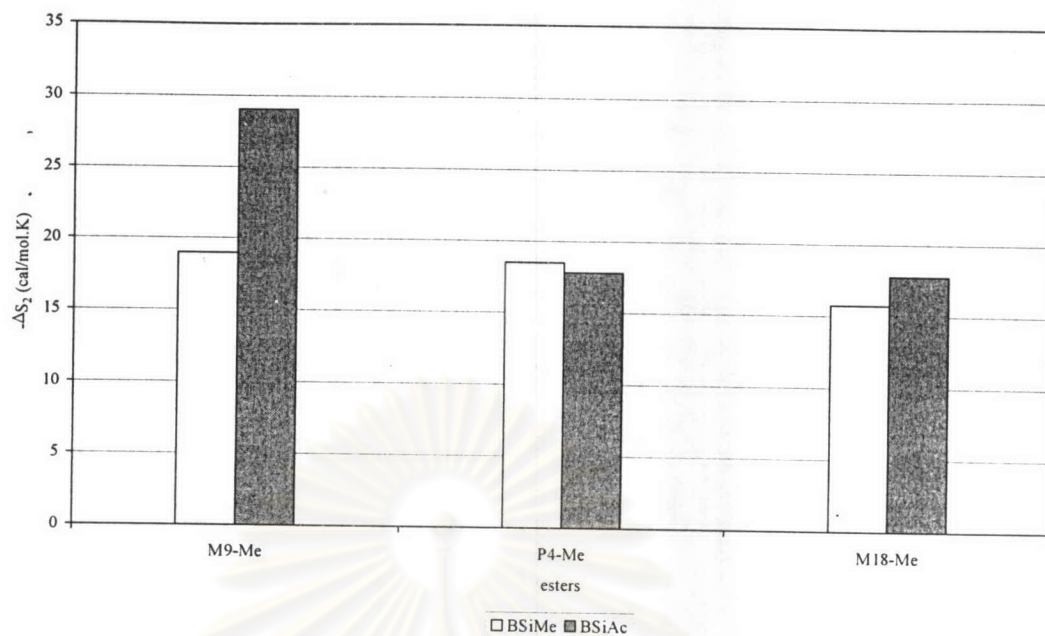


Figure 4.25 Entropy values for second-eluted enantiomers of esters (series 4) on BSiMe and BSiAc columns

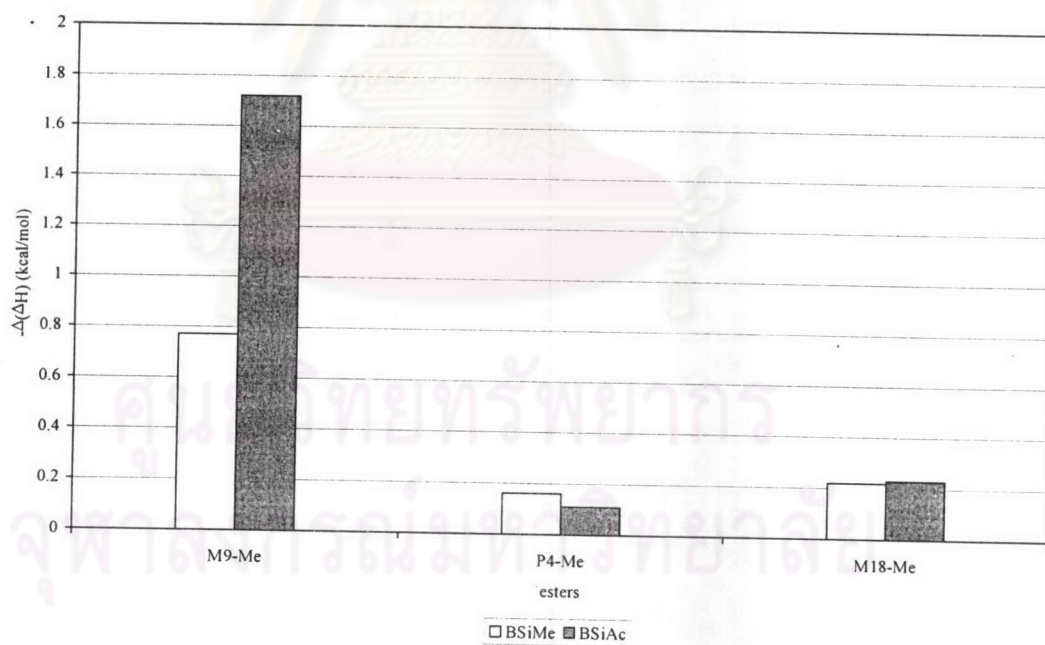


Figure 4.26 Differences in enthalpy values for enantiomers of esters (series 4) on BSiMe and BSiAc columns

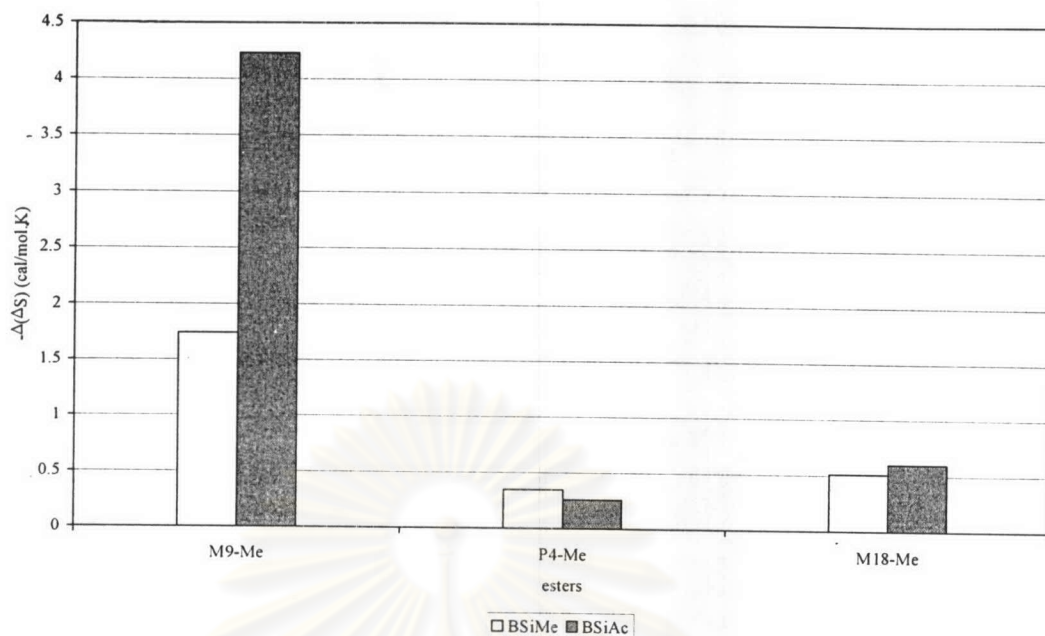
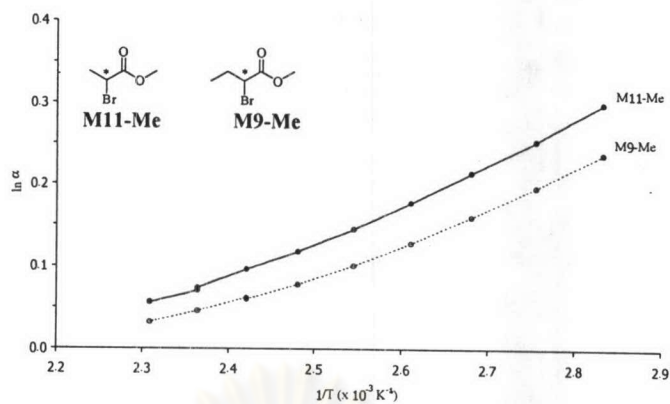


Figure 4.27 Differences in entropy values for enantiomers of esters (series 4) on BSiMe and BSiAc columns

Comparing the enantioselectivity of two structurally similar bromo-substituted esters, **M11-Me** (series 3) and **M9-Me** (series 4) on both columns, it can be seen that the resolution of two esters on two stationary phases is very different. While BSiMe phase exhibited similar enantioselectivity for both esters with slightly greater separation of **M11-Me**, BSiAc phase displayed exceptional separation towards **M9-Me** than **M11-Me**. As seen from figure 4.28, the slopes of  $\ln \alpha$  vs.  $1/T$  curves (a) of **M11-Me** and **M9-Me** are similar. However, enantioselectivity of **M9-Me** on BSiAc phase increases more rapidly as temperature is decreased than **M11-Me**, resulting in significantly greater separation of **M9-Me** at lower temperature (b). This clearly indicates that even a slight difference in the analyte structure can cause a large variation in selectivity.

(a)



(b)

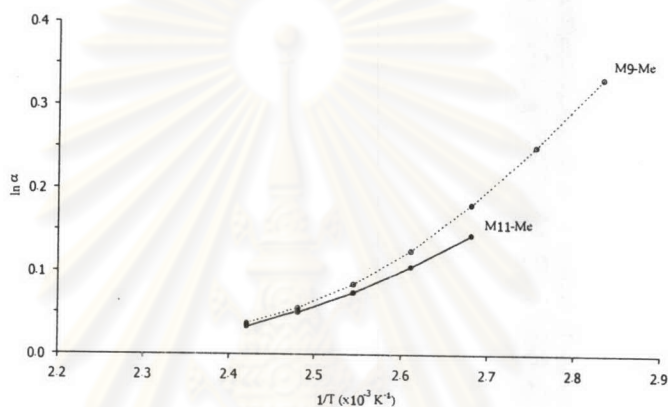
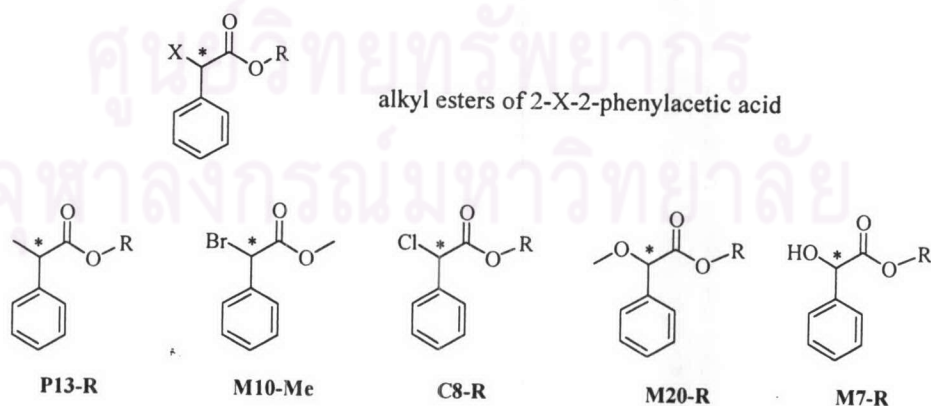


Figure 4.28 Comparison of  $\ln \alpha$  vs.  $1/T$  plots of **M11-Me** and **M9-Me** on (a) BSiMe and (b) BSiAc columns

#### 4.3.5 Esters with different types of substituents, alkyl esters of 2-X-2-phenylacetic acid (Series 5)



This series incorporates methyl and ethyl esters of 2-X-2-phenylacetic acid ( $X = \text{Cl}, \text{Br}, \text{OH}, \text{OMe}, \text{Me}$ ). In this group, the influence of substituent type at 2-position and alkyl ester chain of these esters can be studied.



Because of peak tailing effect, the separation data of **M7-R** on BSiAc column are unavailable. Figures 4.29 – 4.32 show the enthalpy and entropy results for enantiomers of esters in this group on two columns.

In general, on BSiMe phase, lengthening ester chain slightly increases the interaction of ester analytes with the phase. Enantiomer separations of these alkyl analytes, on the other hand, did not have a similar trend. Unlike the enantioseparations of **C8-R** and **P13-R**, the chiral recognitions of **M7-R** and **M20-R** are better when changing ester function from methyl to ethyl. In addition to the alkyl chain length, the interaction and the enantioselectivity of these esters are also dependent on the type of substituent at  $\alpha$ -position of ester molecules. Among all analytes, there are slight differences in the interaction strength and interaction sites while enantioseparation are significantly different.

According to figures 4.31-4.32, the two halogen-substituted esters exhibited high  $-\Delta(\Delta H)$  and  $-\Delta(\Delta S)$  values on BSiMe phase. It appears that by changing halogen substituent from chloro (**C8-Me**) to bromo (**M10-Me**), the resolution rises approximately in double. This suggests that increasing the size of halogen results in greater discrimination between two enantiomers, similar to the findings observed with esters in series 3. Moreover, polar interactions seem to be important factors in the chiral recognition. Considering the separation of **P13-R**, **M20-R**, and **M7-R**, **P13-R** possesses the lowest enantioselectivity owing to the lack of additional interaction between methyl substituent and methoxy groups on BSiMe.

On BSiAc phase (figures 4.29-4.30), changing ester chain from methyl to ethyl results in a little stronger interaction, except for **M20-R**, while enantioselectivities of all analytes decrease with longer alkyl chain. Similar to the results on BSiMe phase, the enantioseparation on this phase depends on substituent types as well. However, enantioselectivities of ester analytes on two chiral columns are very different (figures 4.31- 4.33).

As seen from figure 4.33, the separations of **M20-Me** on both columns are not much different, which contradicts thermodynamic results (figures 4.31-4.32). This is because the figure 4.33 shows the separation at only a given

temperature. On the contrary, thermodynamic parameters exhibit the results over the whole range of data.

The great difference in enantioseparation of analytes on BSiMe and BSiAc columns is possibly due to the differences in substitution at C-2 and C-3 of cyclodextrin molecule which results in different characteristics of these two phases. Firstly, substitution of methoxy by acetoxy increases the polarity of cyclodextrin rim and consequently leads to additional polar interaction between acetoxy on BSiAc and polar substituent on ester molecule. This results in a great change in enantioselectivity of **M20-Me** on BSiMe and BSiAc column. Compared with **P13-Me** ( $\mu_{C-CH_3} = 0.0$  [44]), **M20-Me** ( $\mu_{C-OMe} = 1.28$  [44]) exhibits the different enantioseparation on these two phases. The greater enantioselectivity of **M20-Me** on BSiAc can be ascribed to additional dipole interaction between acetoxy groups on BSiAc and methoxy at 2-position of **M20-Me**. However, ethyl esters of both **P13-Et** and **M20-Et** show almost identical  $-\Delta(\Delta H)$  and  $-\Delta(\Delta S)$  values on BSiMe and BSiAc columns.

Secondly, the cyclodextrin C2-3 opening decreases when changing substituents at C-2 and C-3 of glucose units from methoxy to acetoxy due to steric hindrance. This makes the size of substituent of ester important for the separation. Considering the two halogen-substituted esters, the  $-\Delta(\Delta H)$  and  $-\Delta(\Delta S)$  values of chloro-substituted ester are larger than bromo-substituted ester. This indicates that the chiral recognition of enantiomers on BSiAc phase decreases with increasing the size of halogen substituent. In this case (Br and Cl substituent), the effect of substituent size rather than its polarity dominates the chiral separation on BSiAc column, as can be seen from a great difference in size of chloro (0.99 Å) and bromo (1.14 Å) but a similarity in polarity ( $\mu_{C-Br} = 1.82$ ,  $\mu_{C-Cl} = 1.87$  [44]).

จุฬาลงกรณ์มหาวิทยาลัย



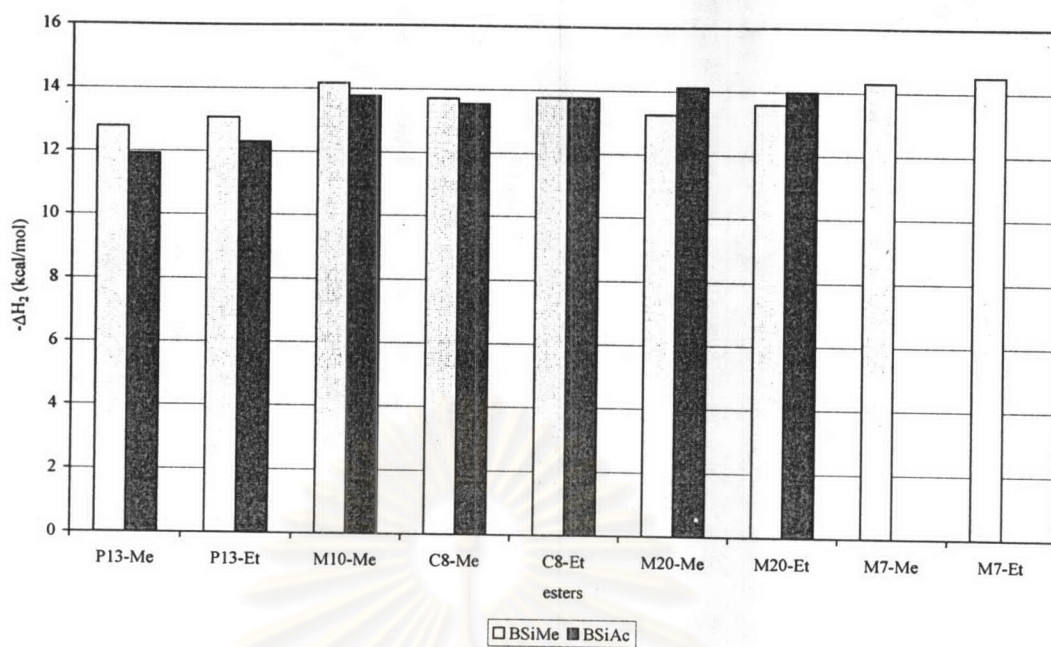


Figure 4.29 Enthalpy values for second-eluted enantiomers of esters (series 5) on BSiMe and BSiAc columns

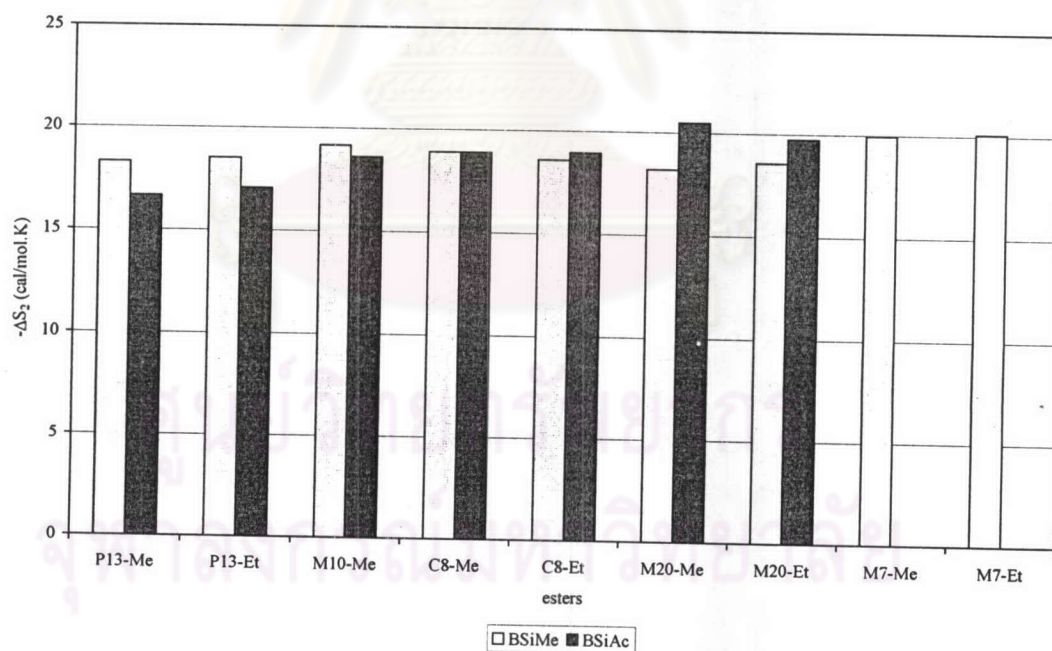


Figure 4.30 Entropy values for second-eluted enantiomers of esters (series 5) on BSiMe and BSiAc columns



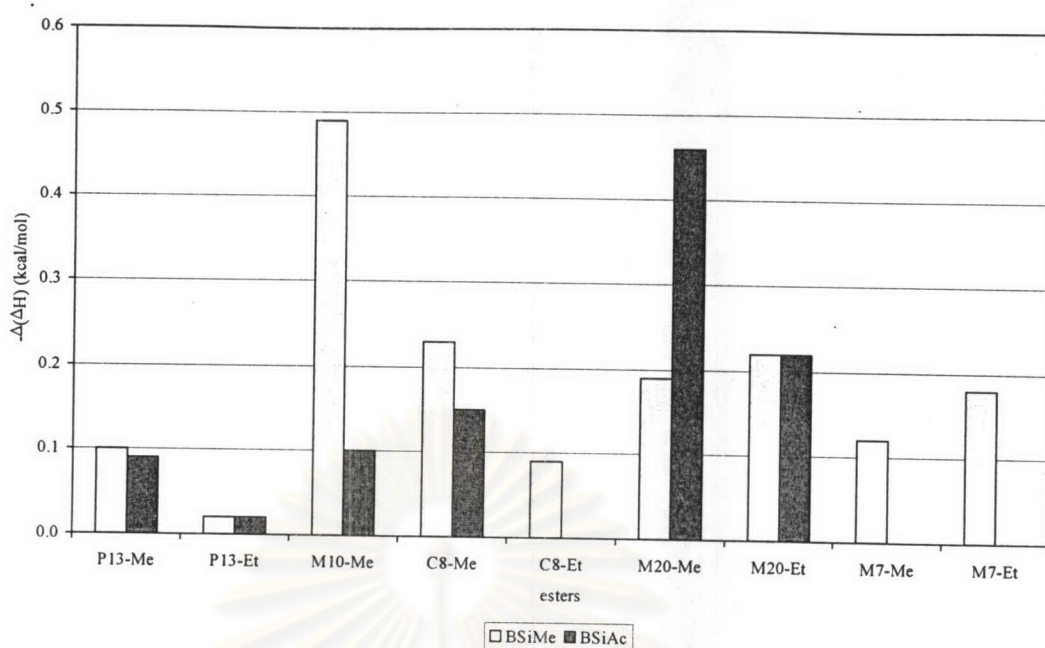


Figure 4.31 Differences in enthalpy values for enantiomers of esters (series 5) on BSiMe and BSiAc columns

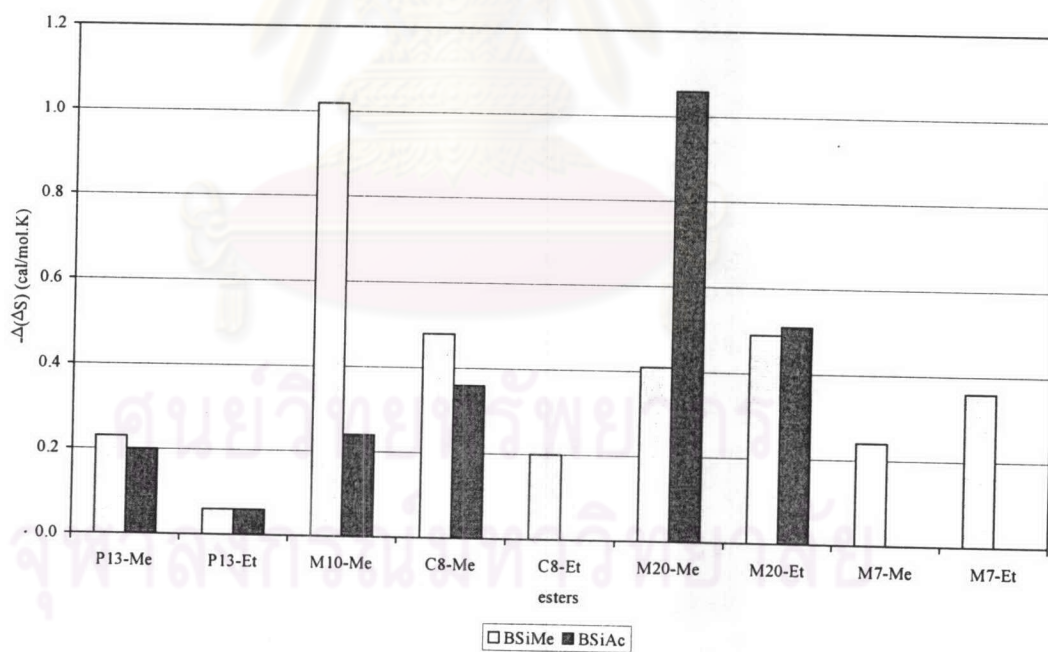


Figure 4.32 Differences in entropy values for enantiomers of esters (series 5) on BSiMe and BSiAc columns

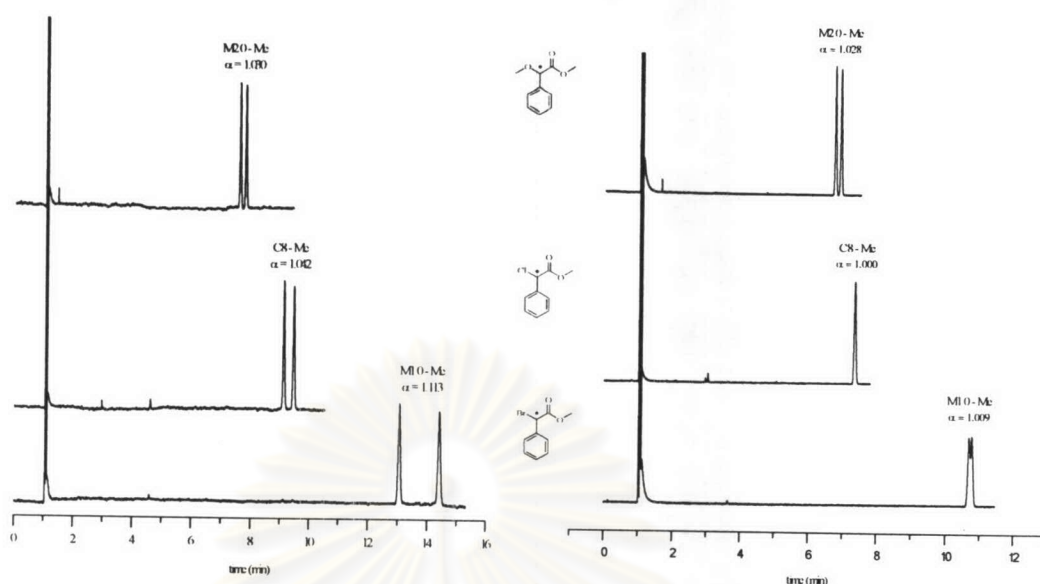


Figure 4.33 Comparison of separations of **M10-Me**, **C8-Me**, and **M20-Me** on BSiMe (left) and BSiAc (right) columns at 130 °C

Comparing phenyl analogues (**C8-Me**, **M10-Me**, **M7-Me**) in this series to methyl analogues (**M12-Me**, **M11-Me**, **M17-Me**) in series 3, it was obvious that the phenyl substituent causes stronger interaction but decreases enantioselectivity substantially in both columns. The stronger interaction of phenyl-substituted ester is likely due to hydrophobic interaction between phenyl and OV-1701 phase. However, steric hindrance of the molecule itself may impede enantiomers to enter deeply into the cavity or to interact with CD molecule. The separations of **C8-Me** and **M10-Me** are compared with those of **M12-Me** and **M11-Me** on BSiMe column in figures 4.34-4.35.

จุฬาลงกรณ์มหาวิทยาลัย

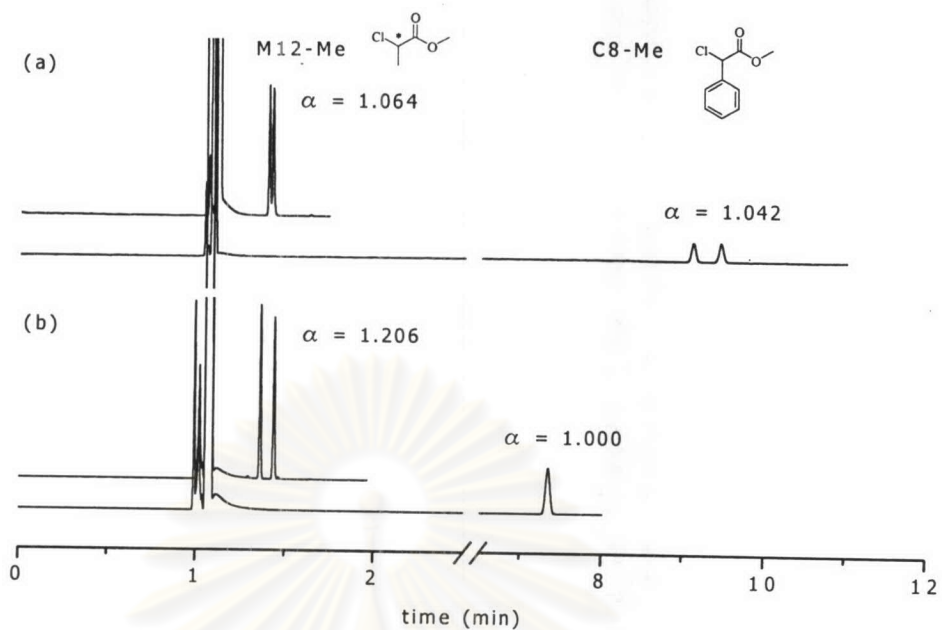


Figure 4.34 Comparison of the separations of **C8-Me** with **M12-Me** at 130 °C on (a) BSiMe and (b) BSiAc columns

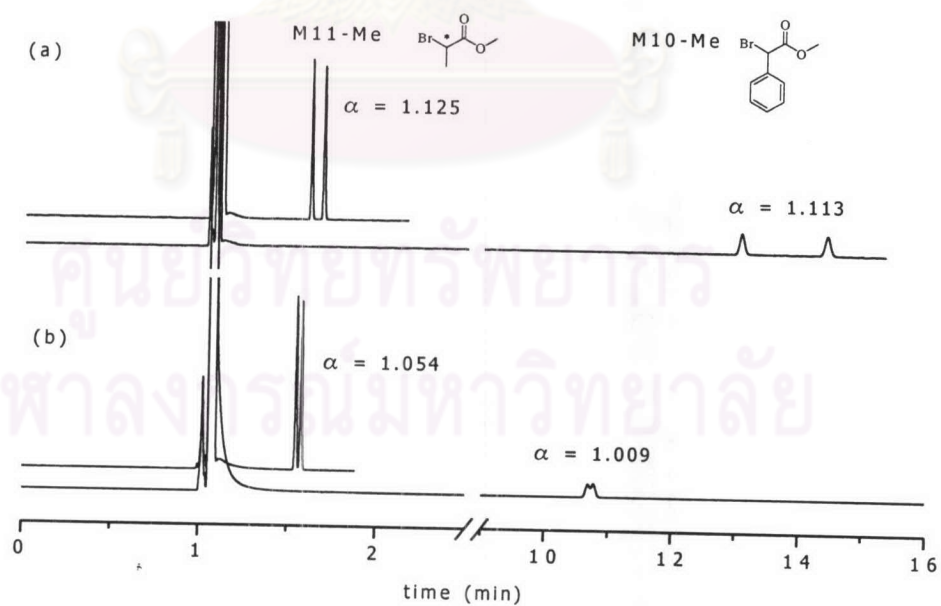


Figure 4.35 Comparison of the separations of **M10-Me** with **M11-Me** at 130 °C on (a) BSiMe and (b) BSiAc columns



#### 4.4 Thermodynamic investigation by *Schurig approach*

As mentioned in chapter II, in this method, thermodynamic parameters are calculated from the plot of  $\ln R'$  (retention increment) versus  $1/T$ . In this study,  $R'$  was obtainable from relative retention factors ( $k'$ ) of enantiomers with respect to *n*-heptane ( $C_7$ ) standard, which has rather weak interaction towards both chiral columns and a polysiloxane column. However, the accurate retention of  $C_7$  could not be determined at high operating temperatures. For this reason, the Kovats plots of  $\log t'$  (adjusted retention time) vs.  $n$  ( $n$  = number of carbon atoms) for a homologous series of *n*-alkanes at various temperatures were constructed. Retention data of  $C_7$  at a desired temperature were estimated by extrapolation of these plots.

The determination of thermodynamic data by *Schurig approach* was carried out for the separation of ester analytes only on BSiAc column owing to random data points on BSiMe column. However, the calculation of thermodynamic data for BSiAc column was not possible for some esters because of non-linearity of the plots, possibly resulted from the nonideal behaviour of  $C_7$ . With BSiAc phase, however, the plots of  $\ln R'$  versus  $1/T$  were not strictly linear. Enthalpy and entropy results for some esters were solely calculated from the linear part of the plots (not the whole temperature range examined). Comparison of thermodynamic data calculated from *van't Hoff approach* and *Schurig approach* is illustrated in table 4.2.

In general,  $-\Delta H$  and  $-\Delta S$  values calculated using *Schurig approach* are lower than those calculated using *van't Hoff approach*. However,  $-\Delta(\Delta H)$  and  $-\Delta(\Delta S)$  values obtained from *Schurig approach* are much higher than those obtained from *van't Hoff approach*. Moreover, trends in those thermodynamic data for each series from both methods are greatly different. Theoretically, the results of *Schurig approach* should be more correct than those of *van't Hoff approach* since the thermodynamic values obtained from *Schurig approach* will not depend on CD concentration or type of polysiloxane used. However, *van't Hoff approach* provided thermodynamic results in better agreement with chromatographic results than *Schurig approach*. For example, according to gas chromatographic separation results,  $\alpha$  values of **P3-R** decreased with lengthening alkyl chain. Considering  $-\Delta(\Delta H)$  and  $-\Delta(\Delta S)$  values obtained from both methods, the trend in enantioselectivity of

*van't Hoff approach* is in agreement with the trend in  $\alpha$  values while *Schurig approach* shows the opposite trend. Another example is **M11-Me** and **P13-Me**. The chromatographic results revealed that **M11-Me** ( $\alpha_{120^\circ\text{C}} = 1.077$ ) could be separated better than **P13-Me** ( $\alpha_{120^\circ\text{C}} = 1.009$ ). However, enantioselectivity of **P13-Me** was greater than that of **M11-Me**, according to *Schurig approach*. More correctly, the reverse result obtained from *van't Hoff approach* showed that **M11-Me** possessed higher enantioselectivity than **P13-Me**.

These discrepancies between chromatographic data and thermodynamic data calculated with *Schurig approach* are probably due to the following reasons. The plots of  $\ln R'$  versus  $1/T$  were not strictly linear. Only linear parts of these plots were used to calculate entropy and enthalpy values. Consequently, there were too small data points used for the calculation of thermodynamic data. Another reason is that the reference standard ( $C_7$ ) may not behave as a truly inert reference. It probably interacts to a certain degree with CD derivatives.



ศูนย์วิจัยทรัพยากร  
จุฬาลงกรณ์มหาวิทยาลัย

Table 4.2 Comparison of thermodynamic parameters obtained from *van't Hoff approach* and *Schurig approach*

| compound             | <i>van't Hoff approach</i> |               |                     |                     | <i>Schurig approach</i> |               |                     |                     |
|----------------------|----------------------------|---------------|---------------------|---------------------|-------------------------|---------------|---------------------|---------------------|
|                      | $-\Delta H_2$              | $-\Delta S_2$ | $-\Delta(\Delta H)$ | $-\Delta(\Delta S)$ | $-\Delta H_2$           | $-\Delta S_2$ | $-\Delta(\Delta H)$ | $-\Delta(\Delta S)$ |
| <b>P3-Me</b>         | 13.29                      | 18.90         | 0.19                | 0.44                | 4.43                    | 11.25         | 0.96                | 2.23                |
| <b>P3-Et</b>         | 13.68                      | 19.22         | 0.15                | 0.36                | 7.25                    | 18.50         | 1.00                | 2.37                |
| <b>P3-<i>i</i>Pr</b> | 13.87                      | 19.46         | 0.14                | 0.33                | 6.63                    | 17.47         | 1.23                | 2.93                |
| <b>P3-<i>n</i>Pr</b> | 14.25                      | 19.66         | 0.10                | 0.25                | 6.66                    | 17.20         | 1.29                | 3.16                |
| <b>M6-Me</b>         | 12.85                      | 17.96         | 0.00                | 0.00                | 5.40                    | 14.00         | 0.00                | 0.00                |
| <b>M11-Me</b>        | 13.79                      | 24.14         | 0.79                | 1.84                | 11.13                   | 24.61         | 0.88                | 1.94                |
| <b>M11-Et</b>        | 12.03                      | 19.59         | 0.14                | 0.34                | 9.51                    | 22.01         | 0.50                | 1.22                |
| <b>M12-Me</b>        | 14.83                      | 27.23         | 2.04                | 4.64                | 12.08                   | 26.16         | 2.03                | 4.28                |
| <b>M12-Et</b>        | 12.83                      | 22.19         | 1.07                | 2.50                | 10.60                   | 23.99         | 1.41                | 3.11                |
| <b>P2-Me</b>         | 14.11                      | 20.61         | 0.65                | 1.50                | 9.34                    | 22.25         | 2.25                | 5.03                |
| <b>P2-Et</b>         | 13.87                      | 19.64         | 0.40                | 0.92                | 7.71                    | 19.13         | 2.15                | 4.88                |
| <b>P13-Me</b>        | 11.93                      | 16.65         | 0.09                | 0.20                | 5.23                    | 13.95         | 1.25                | 3.06                |
| <b>M9-Me</b>         | 14.13                      | 24.60         | 1.36                | 3.25                | 10.55                   | 24.68         | 1.61                | 3.54                |
| <b>M18-Me</b>        | 10.09                      | 17.77         | 0.23                | 0.60                | 6.43                    | 17.27         | 0.64                | 1.62                |
| <b>M10-Me</b>        | 13.77                      | 18.62         | 0.10                | 0.24                | 5.44                    | 4.22          | 0.11                | 0.26                |
| <b>C8-Me</b>         | 13.55                      | 18.90         | 0.15                | 0.36                | 5.71                    | 13.74         | 1.23                | 3.00                |
| <b>M20-Me</b>        | 14.14                      | 20.49         | 0.46                | 1.06                | 7.94                    | 19.28         | 1.93                | 4.43                |
| <b>M20-Et</b>        | 14.00                      | 19.75         | 0.22                | 0.51                | 6.52                    | 16.70         | 1.69                | 4.01                |

$-\Delta H_2$  and  $-\Delta(\Delta H)$  : kcal/mol

$-\Delta S_2$  and  $-\Delta(\Delta S)$  : cal/mol.K